Biogeosciences Discuss., 9, 10149–10205, 2012
www.biogeosciences-discuss.net/9/10149/2012/
doi:10.5194/bgd-9-10149-2012

Biogeosciences Discussions

Remote sensing of LAI, chlorophyll and leaf nitrogen pools of crop- and grasslands in five European landscapes

E. Boegh[1], R. Houborg[2], J. Bienkowski[3], C. F. Braban[4], T. Dalgaard[5], N. van Dijk[4], U. Dragosits[4], E. Holmes[1], V. Magliulo[6], K. Schelde[5], P. Di Tommasi[6], L. Vitale[6], M. R. Theobald[4,7], P. Cellier[8], and M. Sutton[4]

[1]Roskilde University, Dept. of Environmental, Social and Spatial Change, Roskilde, Denmark
[2]Joint Research Centre, Ispra, Italy
[3]Institute for Agricultural and Forest Environment, Polish Academy of Sciences, Poznan, Poland
[4]Centre for Ecology and Hydrology, Edinburgh Research Station, Penicuik, UK
[5]Aarhus University, Dept of Agroecology, Tjele, Denmark
[6]CNR ISAFoM, Napoli, Italy
[7]Technical University of Madrid, E.T.S.I Agrónomos, Madrid, Spain
[8]INRA, UMR 1091 Environnement et Grandes Cultures, France

Received: 10 July 2012 – Accepted: 11 July 2012 – Published: 2 August 2012

Correspondence to: E. Boegh (eboegh@ruc.dk)

Published by Copernicus Publications on behalf of the European Geosciences Union.

Abstract

Leaf nitrogen and leaf surface area influence the exchange of gases between terrestrial ecosystems and the atmosphere, and they play a significant role in the global cycles of carbon, nitrogen and water. Remote sensing data from satellites can be used to estimate leaf area index (LAI), leaf chlorophyll (CHL_l) and leaf nitrogen density (N_l). However, methods are often developed using plot scale data and not verified over extended regions that represent a variety of soil spectral properties and canopy structures. In this paper, field measurements and high spatial resolution (10–20 m) remote sensing images acquired from the HRG and HRVIR sensors aboard the SPOT satellites were used to assess the predictability of LAI, CHL_l and N_l. Five spectral vegetation indices (SVIs) were used (the Normalized Difference Vegetation index, the Simple Ratio, the Enhanced Vegetation Index-2, the Green Normalized Difference Vegetation Index, and the green Chlorophyll Index) together with the image-based inverse canopy radiative transfer modelling system, REGFLEC (REGularized canopy reFLECtance). While the SVIs require field data for empirical model building, REGFLEC can be applied without calibration. Field data measured in 93 fields within crop- and grasslands of five European landscapes showed strong vertical CHL_l gradient profiles in 20 % of fields. This affected the predictability of SVIs and REGFLEC. However, selecting only homogeneous canopies with uniform CHL_l distributions as reference data for statistical evaluation, significant ($p < 0.05$) predictions were achieved for all landscapes, by all methods. The best performance was achieved by REGFLEC for LAI ($r^2 = 0.7$; rmse = 0.73), canopy chlorophyll content ($r^2 = 0.51$; rmse = 439 mg m^{-2}) and canopy nitrogen content ($r^2 = 0.53$; rmse = 2.21 g m^{-2}). Predictabilities of SVIs and REGFLEC simulations generally improved when constrained to single land use categories (wheat, maize, barley, grass) across the European landscapes, reflecting sensitivity to canopy structures. Predictability further improved when constrained to local (10×10 km^2) landscapes, thereby reflecting sensitivity to local environmental conditions. All methods showed different predictabilities for land use categories and landscapes. Combining the best methods, LAI, canopy chlorophyll content (CHL_c) and canopy nitrogen content (N_c) for the five landscapes could be predicted with improved accuracy (LAI rmse = 0.59; CHL_c rmse = 346 g m^{-2}; N_c rmse = 1.49 g m^{-2}). Remote sensing-based results showed that the vegetation nitrogen pools of the five agricultural landscapes varied from 0.6 to 4.0 t km^{-2}. Differences in nitrogen pools were attributed to seasonal variations, extents of agricultural area, species variations, and spatial variations in nutrient availability. Information on N_l and total N_c pools within the landscapes is important for the spatial evaluation of nitrogen and carbon cycling processes. The upcoming Sentinel-2 satellite mission will provide new multiple narrow-band data opportunities at high spatio-temporal resolution which are expected to further improve remote sensing predictabilities of LAI, CHL_l and N_l.

1 Introduction

Nutrient availability is highly variable and related to land use, farming systems, soil type and topography (Duretz et al., 2011) as well as the atmospheric deposition of ammonia and nitrogen oxides (Churkina et al., 2010). Despite a nitrogen-use surplus in European croplands (Eurostat, 2012) which is one of the main causes for European agriculture to be a net source of greenhouse gases (Ciais et al., 2010), water and nutrient resource availability is responsible for large inter-plant-species spatial variation in photosynthetic capacity and carbon exchange rates (Moors et al., 2010). This causes the carbon balance of fields to vary between being a source or a sink (Ciais et al., 2010). Remote sensing-based spectral vegetation indices (SVIs) calculated from broadband satellite sensors have been used to represent the resource constrained Leaf Area Index (LAI) and light absorption for photosynthesis modelling (Field et al., 1995; Zhao, M. S. et al., 2005). However, the maximum light-use efficiencies as well as the maximum Rubisco capacities, which are catalyzing the CO_2 fixation, can vary by a factor of 2 for European crops (Chen et al., 2011; Moors et al., 2010). Because the bulk of leaf nitrogen is associated with Rubisco, leaf nitrogen is considered a critical determinant of the maximum

Rubisco capacity in photosynthesis modeling (e.g. Farquhar et al., 1980; dePury and Farquhar, 1997; Boegh et al., 2002; Kattge et al., 2009), and it also plays an important role for the NH_3 exchange between vegetation and the atmosphere (Mattson et al., 2009; Massad et al., 2010), which is an important component of the nitrogen (N) cycle and closely coupled to the carbon cycle. Due to the characteristic spectral signature of leaf pigments and their N contents, remote sensing of leaf chlorophyll (CHL_l) and leaf nitrogen (N_l) is feasible (e.g. Blackburn, 1998; Broge and LeBlanc, 2000; Boegh et al., 2002; Hansen and Schjoerring, 2002; Sims and Gamon, 2002; Gitelson et al., 2005; Zhao, D. L. et al., 2005; Houborg and Boegh, 2008; Houborg et al., 2009; Dash et al., 2010; Main et al., 2011; Peng and Gitelson, 2012), and it has been found that such products can be used as measures of the light-use-efficiency (Houborg et al., 2011; Peng and Gitelson, 2012) and the maximum Rubisco capacity (Boegh et al., 2002) in photosynthesis modeling.

Most remote sensing-based methods for estimating CHL_l and N_l were developed for single species using leaf-scale data to develop SVIs that are closely correlated with CHL_l and N_l (e.g. Sims and Gamon, 2002; Zhao, D. L. et al., 2005; Main et al., 2011). As for CHL_l, remote sensing of N_l performs best in the visible spectral bands. Its estimation can be indirect due to N_l association with CHL_l (Yoder and Pettigrew-Crosby, 1995), however nitrogen is also included in other pigments such as carotenoids and anthocyanin which have different spectral signatures than CHL_l (Sims and Gamon, 2002). In the absence of nitrogen plants degrade their chlorophyll molecules and CHL_l is determined by the availability of N_l (Filella et al., 1995), thereby causing a close relationship between CHL_l and N_l measurements (e.g. Boegh et al., 2002; Zhao, D. L. et al., 2005). Physiological investment of nitrogen in light-harvesting chlorophyll and Rubisco aims to maximize photosynthesis, and the nitrogen partitioning of leaves between CHL_l and Rubisco is therefore light-dependent and varies with plant growth form and between species (e.g. Hallik et al., 2012). For instance, leaves grown at high light intensity tend to allocate more nitrogen to Rubisco, therefore increasing the photosynthetic capacity per leaf area, whereas shade-tolerant species tend to have higher CHL_l-N_l ratios.

Photosynthesis optimization theory suggests that plants will distribute their nitrogen resources in proportion to the light gradient within the canopy (e.g. dePury and Farquhar, 1997). This complicates the evaluation of remote sensing-based canopy CHL_l and N_l estimation methodologies because ground truth measurements are based on leaf scale data. Some remote sensing studies measure CHL_l of the upper leaf, which is then multiplied by the green LAI to represent canopy chlorophyll (CHL_c) content (e.g. Gitelson et al., 2005; Atzberger et al., 2010). Other studies use random sampling (e.g. Darvishzadeh et al., 2008; Dash et al., 2010) or integrate over the canopy height (e.g. Broge and LeBlanc, 2000). Measuring conditions at canopy and regional scales are further complicated by variations in soil background reflectance and canopy structures of the different land cover types, and it is often found that different SVIs have different capabilities for estimating LAI, CHL_l and N_l (e.g. Broge and Leblanc, 2000). Mismatch in the spatial resolution of ground truth field data and satellite based SVIs over extended regions also challenges the evaluation of SVIs (Garrigues et al., 2008; Dash et al., 2010), and many studies have used leaf and canopy radiative transfer models (CRTMs) to study the sensitivity of SVIs when exposed to different external factors at canopy scale (e.g. Carlson and Ripley, 1997; Broge and LeBlanc, 2000; Haboudane et al., 2004). CRTMs are physically-based models that consider soil and leaf properties, stand geometry and clumping for modeling spectral surface reflectance, however the canopy is typically assumed to consist of a homogeneous layer of vegetation, allthough a 2-layer version of the CRTM model, SAIL has been developed (Verhoef and Bach, 2012). Furthermore, very few studies report on the vertical detection footprint of remote sensors (Winterhalter et al., 2012). It is well-known that dense canopies effectively absorb red light, which leads to diminishing reflectance and saturation effect in the red chlorophyll peak absorption band, and that most SVIs saturate at high LAI values (e.g. Yoder and Waring, 1994; Huete, 1988). A recent experiment aimed at detecting the vertical footprint of a red edge SVI to provide information on N_l in a maize canopy showed, however, that the remote sensor was able to detect N_l down to the lowest levels (Winterhalter et al., 2012).

Despite incomplete representation of within-canopy CHL_l and N_l profiles in many remote sensing data and model studies, the sensitivity of canopy reflectance to soil background reflectance and canopy geometry has been clearly demonstrated and points to the need for land cover-specific conversions to estimate LAI from SVIs (Knyazikhin et al., 1998). Furthermore, the incorporation of local soil parameters, describing the linear relationship between red and nearinfrared (NIR) reflectance of bare soils, improve the estimation of canopy "green-ness" (related to the product of LAI and CHL_l) from SVIs (Broge and Leblanc, 2000). Since the empirical "soil-line" parameters depend on both the spectral characteristics of the background and canopy density and geometry, which vary for different soil types and land use classes within landscapes, generalized soil adjusted SVIs have been developed (Huete, 1988; Huete et al., 2002) which show improved relationships with LAI (e.g. Boegh et al., 2002; Houborg and Soegaard, 2004; Huete et al., 2006). However, because SVIs require empirical calibration to assess LAI, CHL_l and N_l, such calibration may not be transferable to other canopies due to variations in soil background and canopy structure. Therefore, methods have been developed to use physically based CRTMs for inverse model estimation of LAI and CHL_l (e.g. Jacquemoud et al., 2000; Darvishzadeh et al., 2008; Houborg et al., 2009; Atzberger and Richter, 2012). The use of CRTMs is attractive because they are able to represent canopy geometry and the various radiometric properties of leaves and soils, and therefore, they do not require calibration. However, CRTMs require many soil and vegetation-specific model parameters, which may be unknown. Due to the number of unknown variables exceeding the number of radiometric variables in the input data, and because different parameter combinations can yield similar spectral reflectance simulations, the model inversion process is mathematically ill-founded (Combal et al., 2002). A priori information about model parameters or the use of additional input data types (hyperspectral or multi-angular data) can be used to constrain the model inversion, however such information may not be available at large spatial scales, and the use of additional radiometric input data can be redundant. Utilization of spatial information content within remote sensing images can be an attractive solution (e.g. Houborg and

Anderson, 2009; Atzberger and Richter, 2012). Houborg et al. (2007) developed an image-based method for LAI and CHL_l mapping which included automatic parameterization of a combined leaf optics-CRTM model (PROSPECT-ACRM). The method identifies bare soil and dense vegetation fields, and the spectral signatures of these fields are then used to constrain the model inversion for class-specific parameterization. Very good results were obtained for LAI (rmse = 0.4–0.7) and CHL_l (rmse = 5–9 $\mu g\,cm^{-2}$) when applied at a regional scale (Houborg et al., 2007; Houborg and Boegh, 2008; Houborg and Anderson, 2009), and even better results were achieved when applied to field scale image data with 1 m spatial resolution (rmse = 0.25 for LAI and 4.4 $\mu g\,cm^{-2}$ for CHL_l) due to the efficient model parameterization scheme (Houborg et al., 2009). The method has been developed into a userfriendly tool, REGFLEC (REGularized canopy reFLECtance), which combines atmospheric and canopy radiative transfer modeling to estimate LAI and CHL_l directly from at-satellite radiance data (Houborg and Anderson, 2009).

1.1 Objectives

The purpose of this paper is to assess the utility of different remote sensing-based methods for regional mapping of CHL_l, N_l and LAI in crop- and grasslands. For this purpose, five SVIs and the REGFLEC model were applied to high spatial resolution (10–20 m) multispectral SPOT satellite images (Astrium, 2012) of five landscapes studied in the EU project NitroEurope (Sutton et al., 2007; Cellier et al., 2011) located in Denmark, Scotland (UK), Poland, The Netherlands and Italy. Field measurements of LAI, CHL_l and N_l were collected for crop- and grasslands in each landscape, and spatial variations in vegetation N pools were quantified using field data and the high spatial resolution SPOT satellite images of the landscapes. The overall aims were (1) to assess the capability of the selected remote sensing methods to quantify LAI, CHL_l and N_l over a large range of environmental conditions in Europe, and (2) to assess the distribution and size of vegetation N pools in the five European agricultural landscapes.

Such information would be valuable to quantify resource availability for photosynthesis modeling and nitrogen budget assessment.

2 Landscape sites

In 2006, arable land for crop production covered 25 % of the European land area, and grassland pastures cover an additional 17 %, which add up to a total European agricultural land area of 2 286 931 km^2 (EEA/ETC-LUSI, 2010). The five study areas each represent an area of $10 \times 10\,km^2$ and are centered on the NitroEurope landscapes. They are geographically located across a European South-North gradient, ranging from 40°30′ N to 56°20′ N and an West-East gradient from 3°14′ W to 16°46′ E (Fig. 1), thereby representing 3 European climate zones: temperate/humid continental (Denmark and Poland), temperate oceanic (The Netherlands and the UK), and warm Mediterranean (Italy) (Peel et al., 2007). The climate zones reflect the agricultural land use patterns of the selected landscape sites, which are dominated by grassland in The Netherlands (NL) and Scotland (UK), grain crops, maize and potatoes in Denmark (DK) and Poland (PL), and maize, vegetables and fruit production in Italy (IT).

At the UK site, agricultural land use comprises upland pasture (38 %) and crop fields (10 %) which are intermixed with peat bogs (38 %), semi-natural grassland, heathland and moorland (22 %) and some woodland (14 %). Agricultural production is dominated by sheep, beef and poultry systems, although the latter does not contribute substantially to agricultural land use and cropping patterns in the landscape, being dependent on feeds brought in from outside the area. The landscape is located in an upland area (280 m a.s.l.), and the prevailing soil types are Dystric Cambisols, Dystric Histosols and Dystric Gleysols (ESDB, 2010), which are indicative of acidic soils.

The Dutch lowland site (NL) is located just 2 m a.s.l. and dominated by cultivated grassland and pasture (79 %). Only a few crop fields (maize) were observed. There is no woodland in the study area, but many tree belts. Urban/suburban land use covers 17 %, and 4 % of the area is taken up by water bodies and inland marshes. In this

region, Gleyic Podzol is the dominant soil type (ESDB, 2010), indicating intermittent water logging.

At the DK site, land use is dominated by croplands (70 %) intermixed with woodland (21 %) and urban/suburban areas (6 %). The dominant crop type in this region is wheat, but winter oilseed rape, barley and maize are also common. The area is a lowland area (60 m a.s.l.), with fertile soils composed by Haplic Podzols and Gleyic Luvisols (ESDB, 2010).

At the Polish site, 76 % of the land area is cultivated by crops, 8 % by grassland, and woodland covers 13 % of the study landscape. Crop fields are generally very small and managed as small family farms, but large fields are observed in the few but large former cooperative farms. The area is located 80 m a.s.l., and soils are classified as Gleyic Luvisols and Gleyic Fluvisols (ESDB, 2010), indicating exposure to intermittent waterlogging.

At the Italian site, agricultural production is dominated by horticulture and dairy buffalo farming. Approximately 90 % of the area is used for cultivation, with 12 % having a complex cultivation pattern. Cultivated areas include vineyards, fruit trees, maize and vegetables. Vegetable fields are row-cropped with up to 1–2 m between rows, and many plastic greenhouses and bare soil fields were observed in the area during the July measurement campaign. The area is located 15 m a.s.l., and the dominant soil type is Eutric Cambisol (ESDB, 2010).

3 Materials and methods

3.1 Satellite data

Multi-spectral high spatial resolution satellite image data representing radiance in the green (0.5–0.59 µm), red (0.61–0.68 µm) and NIR (0.79–0.89 µm) spectra, as measured by the HRG and HRVIR sensors aboard the SPOT-4 and SPOT-5 satellites were acquired within the NitroEurope project and used in this study (Table 1). One satellite

image is available for each landscape for the period 31 May to 21 July 2008, and one additional satellite image is available for the DK site during an intensive measurement campaign for 19 April 2009. Image data are available at a 10 m spatial resolution for most sites, except for UK and the Danish site in 2008 (DK08), where images are available with 20 m resolution. All satellite images were atmospherically corrected using data on aerosol optical depth, ozone and atmospheric precipitable water content from the MODIS and AIRS/AMSU sensors aboard the Terra (EOS AM) and Aqua (EOS PM) satellites. Atmospheric data were acquired as close as possible in time to the acquisition of the SPOT data (Table 1). Surface reflectance is calculated considering directional multiple scattering using the 6SV1 atmospheric radiative transfer model (Kotchenova et al., 2006), which is included in the REGFLEC tool.

3.2 Field data

In each study landscape, field measurements of LAI and SPAD meter indices (related to CHL_l and N_l) or N_l were made in 7–22 fields over 1–2 days within 4–10 days of the relevant satellite image acquisitions, to provide field reference data for evaluating the remote sensing-based SVIs and REGFLEC simulations. Field measurements were conducted in a total of 93 homogeneous field plots (Table 2) within the five landscapes, with each field plot being geographically referenced with an accuracy of 0.5 m using GPS (Trimble Geo XT, Trimble, USA). Plots were generally located in different fields, however at the Italian site, five plots were located within a large experimental maize field exposed to different stress treatments. Each field plot is represented by two subareas of $3 \times 3\,m^2$ located within a $10 \times 10\,m^2$ region of the field.

3.2.1 LAI

LAI was measured with the LAI-2000 instrument (LAI-2000, LiCor, USA) which uses canopy transmission data measured along a transect. Replicate LAI estimation was made in two neighbouring plots, with each LAI estimate being based on 4 light

transmission measurements along a 3 m transect. If the LAI estimates of the 2 transects varied, a third transect was included. In most cases, LAI variation was very low, but in a few cases at the grassland sites in NL, up to 4 transects were included due to spatial variability. In these fields, the average LAI is used to represent the field plot. In the UK landscape, LAI was estimated using light transmission measurements along a 10 m transect.

3.2.2 Chlorophyll and nitrogen

At the UK site, plant sampling was undertaken in the middle 2 m of the 10 m transect within a 50 cm × 50 cm square. Both green leaves and full plants were sampled. For each, total C and N analysis was carried out after weighing and drying, and vegetation N and dry biomass were measured. For conversion to area-based N_l of the natural grasses, a leaf specific weight of $40\,g\,m^{-2}$ was used. In the four other landscapes, non-destructive measurements of CHL_l and N_l were made using hand-held non-destructive SPAD meter measurements. The SPAD meter (SPAD 502-DL, Minolta, USA) emits and measures leaf transmittance in the red (0.6–0.7 µm) and NIR (0.86–1.06 µm) spectra and provides a ratio that is closely correlated with CHL_l and N_l. In order to convert the SPAD index to CHL_l and N_l contents, calibration was conducted on sampled leaves for maize, wheat, barley, oilseed rape, grasses, tomatoes, artichokes and alfalfa. For SPAD meter calibration of tomatoes, artichokes and alfalfa, 10–15 SPAD indices were measured for leaves of different "green-ness", with the samples subsequently analysed in the laboratory for CHL_l and N_l. For SPAD meter calibration of wheat, barley, grass, maize and oilseed rape, SPAD indices were thoroughly measured in the laboratory and leaves cut into small (1–2 cm) pieces for similar SPAD values. Leaf pieces were divided into pools of similar SPAD index ranges (i.e. 6–10, 11–15, ..., 66–70), and each pool was further split into two samples for CHL_l and N_l estimation, respectively. The samples for CHL_l analysis were kept frozen until analysis, while the samples for N_l estimation were oven dried at 80° for 24 h. Chlorophyll ($a + b$) content was extracted using ethanol, and extinction coefficients published by Porra et al. (1989) were used for

the calculation of chlorophyll concentrations. Nitrogen was estimated using a CHNS-O Elemental Analyzer (CE Instruments, UK). Leaf areas were measured using a scanner (EPSON Expression 1680 Professional, Seiko Epson Corporation, US), and specific weights estimated for the same leaf samples were used to convert the mass-based chlorophyll and leaf N concentrations to leaf area based CHL_l and N_l. CHL_l was found to be exponentially related to SPAD values (r^2 = 0.73–0.93), as also shown in other studies, while N_l was linearly related to the SPAD indices (r^2 = 0.62–0.89). Due to the close similarity of SPAD-CHL_l calibration curves for all vegetation types (Fig. 2a), it was decided to use one single calibration curve for all crops. The resulting calibration curve fit all data quite well (r^2 = 0.87), including the few data that were available for artichokes, tomatoes and alfalfa. Excellent agreement was also found when comparing the calibration curve established for this study with that of the same SPAD meter in an independent study (Houborg and Boegh, 2008). This strongly indicates that one single SPAD-CHL_l calibration curve can be used for area-based estimation of chlorophyll over a large range of crop types, even when being at different development stages. It should be noted, however, that the range of leaf specific weights in this study is quite narrow (52–58 g m^{-2}). For N_l, species-specific calibration curves are needed (Fig. 2b). Combining the SPAD-CHL_l and SPAD-N_l calibration curves, the species-specific nitrogen partitioning is clearly illustrated (Fig. 2c). The CHL_l-N_l relationships (Fig. 2c) were used to convert REGFLEC CHL_l simulations to N_l.

In each field plot, 30–70 SPAD meter measurements were conducted depending on the variability of the data. In order to assess the possible impact of vertical CHL_l variability on the total chlorophyll content of the canopy (CHL_c), measurements were conducted on green leaves at 5 heights in the canopy (this was not always possible for the NL grass fields, due to low canopy heights and narrow leaves). At each level, two measurements were conducted on the same leaf to identify deviating data caused by erroneous data resulting from measurement on veins or, for small grass leaves, insufficient leaf cover of the sensor. If one of the paired measurements approached zero, and the other did not, the lower measurement was discarded. Post-processing further

included a power analysis to test the adequacy of sample sizes to represent the mean SPAD index values of the canopies, i.e.

$$n = ((t_\alpha \sigma)/(e\mu))^2 \quad (1)$$

where n is the required number of measurements to achieve 95 % confidence for the mean SPAD index, t_α is the Student value ($\rho < 0.05$), σ is the sample standard deviation, μ is sample mean, and e is the accepted relative error. In total, SPAD meter data were measured in 91 field plots, of which 83 samples satisfied the 10 % error margin, and 54 samples had less than 5 % error. Eight samples with error levels exceeding 10 % were discarded from further analysis. Most (five) of the discarded samples represent grasslands at the NL site. Power analysis was also applied independently to SPAD meter data measured at the three upper measurement levels (ie at relative canopy heights of 0.6, 0.8 and 1.0), and resulted in rejection of the same eight samples.

3.3 Spectral vegetation indices

Five different SVIs were calculated from each of the six satellite images. The Simplified Ratio (SR) and the Normalized Difference Vegetation index (NDVI) were the earliest SVIs to be developed, and are frequently used indices. They are calculated as:

$$SR = \rho_{NIR}/\rho_{red} \quad (2)$$

$$NDVI = (\rho_{NIR} - \rho_{red})/(\rho_{NIR} + \rho_{red}) \quad (3)$$

where ρ is spectral surface reflectance. Despite inherent normalization of NDVI to reduce soil background and atmospheric sensitivity of SR, the NDVI remains sensitive to soil reflectance. A Soil-Adjusted Vegetation Index (SAVI) was developed, which uses a soil-adjustment factor to shift the origin of the NIR-red spectral space and accounts for first-order soil-vegetation interactions and differential NIR and red radiative transfer through a canopy (Huete, 1988). The Enhanced Vegetation Index (EVI) is derived from SAVI and includes a blue spectral band to reduce sensitivity to atmospheric aerosol

contents (Huete et al., 2002). EVI was found to have a good correlation with LAI of agricultural fields (Boegh et al., 2002). Both the NDVI and the EVI are available from the MODIS satellite sensors as global 8-day products at a 1 km resolution. Because many satellites, including the SPOT satellites, do not measure radiance in the blue band, a 2-band EVI index (EVI2, Jiang et al., 2008) was developed, which is closely related to EVI. The EVI2 is calculated as:

$$EVI2 = 2(\rho_{NIR} - \rho_{red})/(\rho_{NIR} + \rho_{red} + 1) \quad (4)$$

Since the strong absorption of red light by the bulk chlorophyll content of dense canopies can cause data saturation in the peak (red) absorption band of chlorophyll, the far-red or green reflectance was found to be more sensitive to canopy scale chlorophyll variations than ρ_{red} (Yoder and Waring, 1994; Gitelson et al., 1996). This led to the proposal of a Green NDVI which uses a green reflectance (ρ_{green}) instead of ρ_{red} and was closely related to CHL_l (Gitelson et al., 1996):

$$GNDVI = (\rho_{NIR} - \rho_{green})/(\rho_{NIR} + \rho_{green}) \quad (5)$$

A related measure, the green Chlorophyll Index (CI) was proposed to estimate the total canopy chlorophyll content (e.g. Gitelson et al., 2005):

$$CI = \rho_{NIR}/\rho_{green} - 1 \quad (6)$$

Many other SVIs for CHL_l or N_l estimation combine three or more narrow band reflectance data in the the red-NIR transition zone of vegetation reflectance (the "red-edge" region), such as the MERIS Terrestrial Chlorophyll Index (MTCI) (Dash et al., 2010). However, such data are not yet available with the spatial resolution and coverage required for the current study.

3.4 The REGFLEC model

REGFLEC (http://www.regflec.com) is an automatic image-based methodology for regional CHL_l and LAI mapping. REGFLEC version 1.0 (Houborg and Anderson, 2009) is

used here, which requires multi-spectral data measured in green, red and NIR bands. REGFLEC combines the atmospheric radiative transfer model 6SV1 (Kotchenova et al., 2006; Vermote et al., 1997), the canopy radiative transfer model ACRM (Kuusk, 2001) and the leaf optical properties model PROSPECT (Baret and Fourty, 1997; Jacquemoud and Baret, 1990) to predict CHL_l and LAI directly from at-sensor radiance data. The strength of the REGFLEC tool is that it estimates vegetation- and soil-specific parameters for mapped soil and vegetation types in the area. Following atmospheric correction of satellite data, the ACRM-PROSPECT model is first run in forward mode to build look-up tables representing relationships between spectral reflectance, CHL_l and LAI. The look-up tables are built using a wide parameter space representative of a full range of soil and vegetation parameters. REGFLEC then identifies bare soil pixels, and the model is run in inverse mode (simulation of surface reflectance) for the bare soil pixels to estimate a single soil reflectance model parameter representative of each soil class. Next, it is run in inverse mode for high NDVI pixels of each vegetation class, to estimate four class-invariant vegetation parameters (leaf structure, leaf angle distribution, fraction of senescent leaves and Markov clumping parameter). Following model parameterization of class-invariant soil and vegetation characteristics, ACRM-PROSPECT is finally run in forward mode for pixel-wise mapping of LAI and CHL_l.

Spectrally homogeneous land cover maps required by the REGFLEC model were produced using the ISODATA unsupervised image classification algorithm of the image analysis software ENVI (ENVI 4.8, Exelis, UK). The number of land cover classes was initially set high and then reduced stepwise until the classification algorithm provided homogeneous classes which visually satisfied the representation of the surveyed fields and other fields in the landscapes. Water bodies, forest, urban/suburban area, roads and railways were further masked using the CORINE land cover map which has a spatial resolution of 100 m (Fig. 1) and the ESRI Streetmap Premium Europe Tele Atlas data set, using buffer zones of one pixel (10 or 20 m). Greenhouses and polytunnels in the IT landscape were visually identified and masked using the SPOT image data.

Soil maps (1 : 1 000 000) from the European Soil Database (ESDB) of the European Soil Data Center (http://eusoils.jrc.ec.europa.eu/) were used as base soil maps for all landscapes except for Denmark, where a more detailed map comprising three classes (instead of two classes in the ESDB map) was available. For the UK site, it was observed that the CORINE category "peat bogs" was not well represented by the European soil map. The high organic content of these soils is likely to influence soil reflectance, and it was therefore decided to add the higher spatial resolution (100 m) CORINE "peat bogs" class as an additional soil class.

The REGFLEC model was run using version 3 of the leaf optical properties model PROSPECT (Baret and Fourty, 1997). The NDVI threshold for intermediate vegetation density was set to 0.65 (used for selecting dense canopy pixels), and the leaf dry matter content was set uniformly to 55 g m^{-2} corresponding to the mean value estimated for leaf samples.

4 Results

4.1 Landscape variations: vegetation index and LAI

The mean and standard deviation (sd) of SPOT NDVI for the crop- and grassland areas within each 10 × 10 km^2 study landscape is shown in relation to the NDVI seasonality represented by MODIS data (Fig. 3). The seasonality appeared quite similar in Denmark and Poland, with the maximal NDVI around 1 June 2008 corresponding to the timing of the SPOT image acquisitions. However, MODIS NDVI time series indicate that harvesting occurs earlier in PL. Also, SPOT NDVI, MODIS NDVI and LAI measurements (Table 3) all indicate larger vegetation cover in DK08 than in PL at the time of satellite imaging, which suggests that crops in PL are in a more mature (senescent) phase. From SPOT ρ_{red}–ρ_{NIR} scatterplots of the agricultural area, a larger data spread occurs in PL compared with DK08 (Fig. 4), which is increasing the sd of NDVI and decreasing the mean NDVI (Table 3). MODIS NDVI slowly increases towards the end of

the year in both Denmark and Poland, due to emergence of autumn-sown crops such as wheat, barley and oilseed rape. However, it takes longer for vegetation cover to re-establish in Poland (Fig. 3), which may be related to variations in land use practice or climate. Abrupt reductions in MODIS NDVI during winter are related to low solar angles and high frequency of overcast weather.

In the early-season SPOT image of DK09, peak NDVI has not yet been reached (Fig. 3), and lower overall vegetation cover is indicated by both NDVI and LAI compared with the DK08 landscape (Table 3). Nevertheless, the highest ρ_{NIR} values are observed in DK09, which indicates the presence of very dense fields (Fig. 4). Field measurements of DK09 crops confirm the high "green-ness" of canopies, which are at an early development stage with no signs of senescence and no significant CHL_l vertical gradient profile (Fig. 5b). In contrast, more than 50 % of the field plots for DK08 show a strong CHL_l vertical gradient profile (Fig. 5a). Two other groupings of high-density (red to dark green colours in Fig. 4) ρ_{red}–ρ_{NIR} data sets occur in the DK09 landscape: one located at the lower boundary line of the ρ_{red}–ρ_{NIR} scatterplot (the "soil-line"), indicating presence of bare soils, and another, located in the intermediate ρ_{NIR} range with relatively low ρ_{red}, indicating the presence of less densely vegetated fields. The mixture of bare fields (maize not yet sown), intermediate density fields (winter-wheat) and very dense fields (winter-oilseed rape) in DK09 results in largely contrasting values in this early-season satellite image.

Other landscapes with high-density soil-line formations (and exposure of bare soils) are the IT and UK sites (Fig. 4). The UK site has a very short soil-line represented by low reflectance data, which likely represents dark organic (peat) soils, whereas the IT site has a much larger data spread (extended red region) along the soil-line, which indicates larger spatial variability in soil background reflectance. The soil line of IT includes very low reflectance data, which is in good agreement with the prevailing cambisols, also called brown soils, of this region. In IT, NDVI is lowest in summertime, and the NDVI seasonality indicates that harvesting takes place 2–3 times per year (Fig. 3). The low NDVI at the time of SPOT satellite imaging agrees with field observations of widely

spaced row-cropped vegetables and bare soil areas. The LAI of such widely spaced tomato fields in IT were not measured and therefore not included in the LAI estimates in Table 3. However LAI of these fields are visually estimated to be < 1 (LAI of one relatively dense tomato field was measured and found to be 1.3). The overall lower vegetation cover of IT is also visualized by the ρ_{red}–ρ_{NIR} scatterplot (Fig. 4), where ρ_{NIR} is clearly lower than for the other landscapes, and the bulk reflectance data (red colours) are indicating a prevalence of bare soils and sparse-to-intermediate vegetation cover.

In the Scottish landscape (UK), the MODIS NDVI time series indicate that vegetation development started later in the year (23 April 2008), compared with the DK and PL landscapes. Vegetation growth accelerated approximately 2 weeks later than in Denmark, and it peaked around 26-June, which was 4–6 weeks later than the peak NDVI of DK. SPOT satellite imaging took place about one month after peak NDVI is reached in UK (Table 1). Despite the clear (high-density) soil-line formation at the UK site indicating presence of bare soil areas, the average NDVI of this site was higher than for all the other landscapes. Compared with the LAI measurements of the UK landscape, MODIS and SPOT NDVI are very high (Fig. 3 and Table 3) which indicates higher vegetation cover of the landscape than indicated by the LAI measurements of the seven field plots (five grassland and two arable fields). NDVI is also sensitive to soil background reflectance, and the low background reflectance of dark (organic-rich) soils tends to increase the NDVI relative to the NDVI of a similar vegetation canopy with a bright soil background (Huete, 1988).

The grasslands of NL are characterized by high NDVI with low seasonal variation. However, NDVI was slightly reduced at the time of the SPOT satellite imaging, which may be indicative of recent grass cutting. A secondary group of high-density reflectance pairs (red colours) in the lower part of the ρ_{red}–ρ_{NIR} scatterplot (Fig. 4) supports the presence of recently cut fields with low residual vegetation cover.

4.2 Landscape variations: chlorophyll and leaf nitrogen

Despite the low vegetation coverage in IT, the vegetables cultivated at this site were characterized by the highest CHL_l and N_l concentrations (Table 3). The largest mean N_l concentrations occured in artichokes (7.82 g m^{-2}), tomatoes (7.05 g m^{-2}) and alfalfa (4.37 g m^{-2}), followed by oilseed rape (3.11 g m^{-2}), wheat and barley (2.22 g m^{-2}), grass (1.54 g m^{-2}) and maize (1.44 g m^{-2}). Measured canopy N contents (N_c) are lowest in the UK landscape, which is dominated by semi-natural grassland, and highest in DK08 (Table 3). The N_c estimate of fields in IT (Table 3) does not fully represent the field sites, due to incomplete representation of LAI for widely spaced row-cropped tomato fields. For CHL_l, oilseed rape had the highest concentrations (mean 842 mg m^{-2}). This was followed by artichokes (743 mg m^{-2}), tomatoes (608 mg m^{-2}), alfalfa (572 mg m^{-2}), wheat and barley (390 mg m^{-2}), potatoes (372 mg m^{-2}) and grasses (340 mg m^{-2}).

Despite coefficients of variation (CV = sd mean^{-1}) in the range 20–35 % for the mean CHL_l of fields within individual landscapes, the averaged within-field variation of CHL_l and N_l exceeded the between-field variability at the DK sites (Table 3). This highlights the importance of a consistent leaf measurement strategy for accurate ground-truth estimation of mean CHL_l.

For nitrogen, the CV for mean N_l of fields range between 8 % and 68 % for the different landscapes. Due to the larger species-specific variations in N_l than CHL_l, between-field variation of mean N_l grossly exceeded the mean within-field variation in N_l at the IT and UK sites. The lowest between-field variability was observed in the DK09 (mostly wheat) and NL (mostly grass) landscapes (Table 3), which were characterized by more uniform land use.

4.3 Within-canopy variations

Three major types of within-canopy vertical CHL_l gradient profiles were evident in the leaf measurements across the European landscapes, which contribute to increase

within-field variability in CHL_l and N_l. Profiles either had CHL_l increasing from bottom to top of the canopy (Fig. 5a), uniform vertical CHL_l distributions (Fig. 5b) or decreasing CHL_l concentrations from bottom to top (Fig. 5c). Linear regression slope coefficients (s) and the coefficients of determination (r^2) describing the relationships between CHL_l data and relative measurements heights (h_r) can be used to indicate whether CHL_l profiles are increasing, decreasing or uniform (Fig. 5). Distributions where CHL_l-h_r regression slopes are characterized by low r^2 are often weakly S-formed or bell-shaped, but are generally characterized by a poor vertical structure (Fig. 5b). In contrast, CHL_l-h_r regression slopes with high r^2 and $s > 0$ (Fig. 3a) or $s < 0$ (Fig. 5c) have strong CHL_l vertical gradient profiles with increasing or decreasing gradients. Defining a strong CHL_l profile as a CHL_l-h_r relationship characterized by $r^2 > 0.68$ ($p < 0.1$), it was found that 20 % of the total fields had strong vertical CHL_l gradient profiles. Increasing CHL_l contents from bottom to top occurred particularly frequently in DK08, where more than 50 % of the fields (barley, wheat) showed strong CHL_l vertical gradient profiles, and in PL (oilseed rape, potatoes, alfalfa and barley), where 34 % of fields showed strong CHL_l vertical gradient profiles. Decreasing ($s < 0$) CHL_l profiles were observed in maize fields in IT and NL. Generally the maize crops with lower canopies had more uniform CHL_l profiles, whereas tall (> 2 m), irrigated and fertilized maize crops had strong "negative" ($s < 0$) CHL_l vertical gradient profiles. CHL_l profiles are more uniform in the early season (19 April) DK09 landscape (only one field showed significant CHL_l vertical gradient profile), however decreasing CHL_l contents in the upper 1–2 measurement levels (h_r = 0.8–1) are normal and contributed to increased within-field CHL_l variability (Table 3).

4.4 Remote sensing-based LAI

Statistically significant relationships ($p < 0.01$) were found between all remote sensing-based LAI predictions (SVIs and REGFLEC simulations) and LAI when considering all LAI data in the landscapes sites (n = 93). The REGFLEC model performed best

(r^2 = 0.62) with a linear regression slope approaching unity (0.99) and a zero intercept. When considering only uniform canopies with no CHL_l vertical gradient profiles (n = 72), the REGFLEC predictability of LAI further improved (r^2 = 0.7). The improved predictability was due to higher statistical correlation in DK08 and PL, where strong positive ($s > 0$) CHL_l vertical gradient profiles frequently occurred. Removal of (maize) canopies with negative ($s < 0$) CHL_l vertical gradient profiles (Fig. 5c) improved the predictability of EVI2 (r^2 increased from 0.75 to 0.8) and REGFLEC (r^2 increased from 0.52 to 0.78) only. The accuracy of REGFLEC LAI predictions for all homogeneous canopies in all the landscapes was given by rmse = 0.73. This is in the lower range of prediction capabilities demonstrated in earlier REGFLEC applications (rmse = 0.4–0.75).

LAI estimates generally improve (Table 4) when restricting the analysis to the major European agricultural land use classes (wheat, maize, barley, grassland) separately, thereby reducing effects due to different canopy structures. Different methods showed the best capabilities for LAI estimation, depending on canopy structure. For homogeneous canopies without significant CHL_l vertical gradient profiles (Table 4), REGFLEC had the highest determination coefficients for wheat (r^2 = 0.75); GNDVI was best for grass (r^2 = 0.83); EVI2 worked best for maize (r^2 = 0.8), and CI had the highest determination coefficient for barley (r^2 = 0.70). The rmse (calculated from measurements and LAI predictions), showed that the best results for the individual land use categories had rmse's ranging from 0.33 to 0.74 (Table 4).

Considering the individual landscapes separately further improved the predictability of REGFLEC and SVIs. This is very likely due to the large range in soil types of the different landscapes (Table 5). The exception to this was for IT, where REGFLEC performed poorly. Poor performance can be due to row crops in this landscape. Row crops does not comply with the homogeneous (turbid medium) canopy representation of CRTMs like ACRM (used by REGFLEC). It may also be due to a lack of image pixels representing dense vegetation of these row-cropped vegetables. The REGFLEC model requires the presence of dense vegetation fields of all land cover classes in order to

parameterize the leaf and canopy properties that are required by the model to simulate LAI and CHL_l. Furthermore, the "background reflectance" of the IT site is very complex, due to some vegetables and fruit trees being covered by nets for pest protection. In contrast to the SVIs, REGFLEC uses image information from the complete landscape, and not only for the field plots, for model parameterization. All SVIs, however gave statistically significant results for LAI mapping of the IT site, and both REGFLEC and the SVIs gave statistically significant results for LAI mapping of all other landscapes. For landscape scale mapping of LAI, r^2 ranged between 0.74 and 0.95, with EVI2 performing best in three out of six landscape images (Table 5). Generally EVI2 appeared to be superior in landscapes comprising a majority of fields with large LAI and/or NDVI, such as DK08, NL and UK (Table 3). REGFLEC performed best when both bare soils and very dense fields were present in the landscape, as was the case for DK09 (Fig. 4), and SR performed best in IT, which is characterized by sparse-to-intermediate vegetation covers.

Combining the methods with the highest r^2 for the individual landscapes (Table 5) increased overall LAI predictability (Fig. 6a) for the six European landscape images (homogeneous canopies only). In this case, 84 % of total data variability could be predicted with a rmse of 0.59 ($n = 72$). Within individual landscapes, rmse varied from 0.22 to 0.67 (Table 5). For comparison, Viña et al. (2011) evaluated the performance of eight SVIs for LAI prediction of two crop types with contrasting canopy structures (maize and soybean) and found values of rmse in the range 0.58–2.53 (median 0.88).

4.5 Remote sensing-based CHL_l and N_l

No significant relationships were found between remote sensing-based predictions (SVIs and REGFLEC simulations) and leaf scale CHL_l or N_l. Statistically significant relationships ($p < 0.05$) were, however, found between all remote sensing-based methods and CHL_c, with REGFLEC having the best overall predictability ($r^2 = 0.34$, $p < 0.001$) when considering all measurement sites ($n = 77$). When restricting the evaluation to canopies with uniform CHL_l vertical gradient profiles ($n = 61$), REGFLEC

predictability improved ($r^2 = 0.51$; $p < 0.0005$). Generally the CV was higher for CHL_c than for LAI at landscape scale (Table 5), and remote sensing-based estimates were generally less well related to CHL_c than to LAI. Only for barley, where field measurements of LAI were mostly high with low variability (Table 4), was the predictability for CHL_c ($r^2 = 0.9$) clearly much better than for LAI ($r^2 = 0.7$). In this case, the chlorophyll index CI was better than the other methods. For the other land use types, where the CV for LAI was larger, predictabilities were generally better for LAI than for CHL_c (Table 4).

For maize (Table 4), and more generally in PL and IT (Table 5), where 30–50 % of field measurements represent maize, predictability of CHL_c was not statistically significant ($p < 0.05$) for any methods. However the predictability for N_c was much better than for CHL_c for maize, and all methods were statistically significantly related to N_c of maize. The predictability for CHL_c of different land use types varied with r^2 between 0.48 and 0.90 whereas the best predictabilities for N_c (all statistically significant) were characterized by r^2 between 0.53 and 0.91 (Table 4).

Overall, REGFLEC had the best capability to predict N_c for all landscapes with r^2 increasing from 0.46 ($n = 83$) to 0.53 ($p < 0.0005$), when the data set was restricted to homogeneous fields without strong CHL_l vertical gradient profiles ($n = 68$). As for the LAI estimations, REGFLEC generally worked best for CHL_c and N_c estimation of wheat. EVI2 worked best for N_c estimation of maize, and CI had the highest r^2 for CHL_c and N_c estimation of the dense barley fields. For grass, REGFLEC gave the best results for CHL_c, whereas CI provided the best results for N_c estimation.

When considering individual landscape sites separately, predictabilities for N_c further increased for most landscapes, except for IT and PL which were characterized by large variations in land use types (Table 2) and large species-dependent N_l variations (Fig. 2). For IT there was a possible correlation ($p < 0.1$) between SR and N_c ($r^2 = 0.4$) while for N_c in PL, the statistical confidence level for the correlation ($r^2 = 0.46$) is just 78 %. For the other landscapes, 70–95 % of N_c data variability could be predicted with high statistical confidence ($p < 0.05$) providing rmse in the range 1.12–1.55 g m^{-2}.

Combining the best methods (Table 5) results in being able to explain 70 % of total CHL_c data variability (Fig. 6b) and 76 % of total N_c data variability (Fig. 6c) within the five European landscapes by the remote sensing methods (homogeneous canopies only). This resulted in rmse of 346 mg m^{-2} for CHL_c and 1.49 g m^{-2} for N_c. Within individual landscapes, rmse varied across the range of 216–397 mg m^{-2} for CHL_c and 1.12–2.35 g m^{-2} for N_c (Table 5). For comparison, Gitelson et al. (2005) found rmse = 320 mg m^{-2} when estimating CHL_c for maize and soybean using an optimal narrow-band red-edge SVI, whereas the use of broad-band (MODIS) reflectance for CI evaluation resulted in rmse = 690 mg m^{-2}. Hansen and Schjoerring (2002) used a partial least square regression technique to identify the best suited spectral bands for N_c prediction. They found that the use of optimal narrow-band NDVI resulted in rmse = 0.8 g m^{-2} for wheat.

4.6 Vegetation nitrogen pools of European landscapes

When different methods are combined, it was possible to explain large variations in LAI, CHL_c and N_c across the European study landscapes (Fig. 6). Model efficiencies (ME) expressed in terms of Sutton-Ratchliffe's coefficient

$$ME = 1 - \sum (p_i - o_i)^2 / \sum (o_i - o_{avg})^2$$

where p_i represents predictions, o_i represents observations, and o_{avg} is the observed mean, confirmed that the spatial predictions were in all cases significantly better than assuming mean values for the land use types: ME = 0.84 for LAI; ME = 0.70 for CHL_c, and ME = 0.73 for N_c. Note, ME = 1 is a perfect prediction, and ME < 0 means that predictions are no better than the mean of the observed data. Maps of N_c predictions further illustrated large spatial variations in land use structure with many small fields responsible for small-scale variations in the vegetation N pools of crop- and grasslands (Fig. 7).

Generally the largest vegetation N pools were found in DK08 and PL whereas the smallest vegetation N pools were found in DK09 and UK (Table 6). However these overall comparisons should be interpreted with care for PL and IT due to the lower statistical confidence of predictions in these landscapes (78 % probability for significant correlation in PL, and 90 % for IT), lower r^2 and larger rmse. Predicted N_c in PL explained only 46 % of data variability and rmse was 1.93. In IT, rmse was even higher (Table 5). The remote sensing-based predictions of mean N_c for PL and IT are however in good agreement with the observed mean N_c (Fig. 8).

Mean N_c based on field measurements tended to exceed the landscape averaged N_c predictions in DK09, UK and NL, but very good agreements are found for the other sites (Fig. 8). In DK09 and NL, lower predicted mean landscape N_c was due to the presence of bare and sparsely vegetated fields (spring sown crops in the early-season DK09 landscape; grass fields cut shortly before the image was taken in NL) while in UK, fewer field measurements were available for comparison of mean values, and the extensive grasslands contribute to the low N_c of this landscape (Fig. 8). The largest predicted mean landscape N_c were found for DK08, IT and PL (with lower confidence in IT and PL) where an average of 5.66 t N_c km^{-2} was estimated for the agricultural area (Table 6). Due to the larger proportion of agricultural area in PL, the total landscape N_c (4.01 t N_c km^{-2}) stored in crops was largest for this study area (Table 6). Large spatial variations were found in both measured and predicted N_c within and between the landscapes which can be attributed to seasonal variations, land use and spatial variations in resource (water and nutrients) availability. Frequency distributions of N_c (Fig. 8) are seen to be negatively skewed in DK08 and PL, indicating prevalence of fields with dense vegetation, and with N_c reaching higher values in DK08 than in PL. N_c distributions are positively skewed in NL and IT with largest spatial variation in IT; and it is strongly positively skewed in DK09 and UK due to the large fractional areas with sparse vegetation (DK09) and/or low N_l contents of grasses (UK). It was not possible to find measured or modelled estimates of N_c in the scientific literature for comparison.

5 Discussion

5.1 Remote sensing predictabilities for LAI, CHL_c and N_c

Generally it is recognized that site- or vegetation-specific empirical corrections or model parameterizations are needed to achieve accurate LAI and CHL_l estimations from regional applications of remote sensing data. These findings are also reflected in the present study where the predictability of SVIs and REGFLEC generally improved when constrained to single land use categories. Predictability improved further when constrained to local ($10 \times 10\,km^2$) landscapes, with the exception of N_c prediction for very heterogenous land use. Even though the REGFLEC model is designed to automatically correct for soil- and vegetation-class specific properties, it was found to perform best in landscapes comprising large contrasts in vegetation cover, ranging from bare soil to dense vegetation, such as for the DK09 study area. For individual landscapes, different methods had different predictabilities. However for each landscape, it was possible to establish statistically significant relationships with LAI using field data representing a variety of land use types. The findings suggest that empirical calibration of SVIs using a variety of data representing different land uses can provide LAI estimates with rmse in the range 0.2–0.7, and that land cover-specific SVIs or calibrations can further improve LAI estimates within individual landscapes. For this purpose, detailed land cover maps representing all vegetation types are needed.

Overall REGFLEC provided the best (statistically significant) LAI, CHL_c and N_c predictions for all six European landscape images with an accuracy for LAI (rmse = 0.73) better than what was found using broad-band SVIs in this and other studies (Atzberger and Richter, 2012; Viña et al., 2012). One reason for the relatively good performance of REGFLEC and SVIs is related to selecting a subset of field data so that only homogeneous canopies without CHL_l vertical gradient profiles were used to evaluate predictions. Strong CHL_l vertical gradient profiles were observed in mature canopies, in particular in DK08 and PL. Removal of canopies with CHL_l vertical gradient profiles fulfills the prerequisites of CRTMs (used by REGFLEC) that leaves should have uniform

properties, and this significantly improved the predictive capability of both REGFLEC and SVIs for the DK08 and PL sites. Removal of maize canopies with "negative" ($s < 0$) CHL_l vertical gradients did not consistently improve the results of the different methods. This may be related to the erectophile structure of maize canopies which allows the remote sensor to measure reflectance at deeper levels in the canopy (Winterhalter et al., 2012). Effects of within-canopy CHL_l variations on surface reflectance is typically not considered in remote sensing studies, but this study showed that it could have a significant effect on the predictability of LAI, CHL_c and N_c. Some CRTMs consider vertical variation in canopy structure using two layers to represent color gradients, clumping and tree crowns (Verhoef and Bach, 2008). Also, so-called functional-structural plant models (Godin and Sinoquet, 2005) are being used to study 3-D interaction between light absorption and biological processes such as canopy growth. However these modelling approaches have focused on representing light scattering effects of canopy structure (e.g. Casa et al., 2010). The sensitivity of surface reflectance to vertical variations in CHL_l and N_l has not been investigated previously and is not known.

Considering the wide range of environmental conditions and land use types across the six European land use cases, the results obtained in this study are relatively encouraging. However, better LAI accuracies (rmse down to 0.4) were obtained in previous REGFLEC applications (Houborg et al., 2007; Houborg and Boegh, 2008; Houborg and Anderson, 2009). Better LAI accuracies were also found by Atzberger and Richter (2012) who used pixel neighborhood information to regularize inverse model predictions of LAI for three crops (rmse = 0.54). Viña et al. (2012) used field-spectrometric data to compare the LAI predictabilities of different SVIs for maize and soybean, and they found that the best results were obtained using a narrow-band red-edge chlorophyll index (rmse = 0.58). The higher accuracies reported for LAI in these studies were however comparable to the rmse of REGFLEC when applied to the DK09 site in the current study (rmse = 0.53). However, even better results were achieved by SVIs in this study in some cases when restricting the evaluation to separate land use categories (Table 4) or individual landscape sites (Table 5). In particular, EVI2 had superior LAI

predictability in three out of six landscape images (DK08, NL and UK) characterized by relatively high NDVIs (Table 3; Fig. 2); SR was superior for LAI prediction of the sparsely vegetated IT site (Table 5), while REGFLEC worked best for DK09 where a large range of vegetation covers was present. Generally, broad-band SVIs are more sensitive to soil background than to accurate parameterization for atmospheric correction of radiance data (Broge and Leblanc, 2000), however uncertainties related to the atmospheric corrections of image data in the different landscapes can be contributing to lower predictability for land use categories across the European landscapes relative to predictabilities within individual landscapes. Such effects could however not be quantified in the present study.

For CHL_c and N_c estimation, field-spectrometric studies based on hyperspectral and narrow-band reflectance data show that CHL_c could be retrieved with rmse of 310–320 mg m^{-2} when considering 1–2 species (Gitelson et al., 2005; Darvishzadeh et al., 2008). However, when including more species, such as in a heterogeneous grassland, rmse increased to 440 mg m^{-2} (Darvishzadeh et al., 2008). This is comparable to the predictability of REGFLEC when applied to the six landscape cases in this study (rmse = 439 mg m^{-2}). Improved accuracies were however found by SVIs and REGFLEC when the evaluation was constrained to distinct land use categories and individual landscapes (Tables 4–5). In this case, the best result for CHL_c prediction (rmse = 117 mg m^{-2}) and N_c prediction (rmse = 0.59 g m^{-2}) were provided by CI for barley fields.

The better results for CHL_c prediction compared with LAI prediction of barley fields (best by CI) may be due to LAI generally being high with low variation. In this case the reflectance may be more sensitive to variations in leaf chlorophyll, xanthophyll and (for the green band used in CI and GNDVI) anthocyanin. For all other vegetation types, the range of LAI data was higher, and the predictability for LAI was better than for CHL_c and N_c. Darvishzadeh et al. (2008) also found that predictability for LAI was better than for CHL_c (using inverse radiative modelling of hyperspectral data), but that CHL_c predictability exceeded LAI predictability when the number of species was increased.

This is however not the case in the current study where landscape predictability of LAI was better than that for the different land use categories, due to the large variations in environmental conditions across the European landscapes.

Some studies have found that leaf scale chlorophyll can be predicted from image data with rmse in the range 4–9 µg cm^{-2} (Houborg and Boegh, 2008; Houborg and Anderson, 2009; Atzberger and Richter, 2012). Even though REGFLEC has shown such capabilities in previous studies, it was not possible to achieve statistical confidence ($p < 0.05$) for CHL_l prediction in this study. This may have been due to insufficient bare soil pixels in the growing season to establish a robust soil parameterization for each soil class. In this case, a solution could be to include a satellite image from before the growing season to improve the soil parameterization, as shown by Houborg and Boegh (2008). Another requirement, the presence of dense vegetation cover of each land use class, was not fulfilled at the IT site.

The use of narrow-band indices for a single species (without variations in soil background) has given significantly better estimates for N_c than those found for the separate land use categories in this study (rmse = 0.66–2.38 g m^{-2}). For instance, Fitzgerald et al. (2010) applied three spectral bands in the red-edge zone to a triangular SVI approach and found that N_c of wheat could be retrieved with rmse = 0.65 g m^{-2}. Hansen and Schjoerring (2002) used an optimal narrow-band NDVI to achieve N_c for wheat with rmse = 0.8 g m^{-2}. Landscape scale estimates of N_c in this study resulted in rmse = 1.12–1.66 g m^{-2} for DK08, DK09, UK and NL. For IT and PL, N_c estimates were obtained with lower statistical confidence and larger rmse (1.93–2.35 g m^{-2}) due to large land use heterogeneity.

While similar CHL_l regression equations could be established for different crops using leaf scale absorbance data measured by the SPAD meter, remote sensing-based N_l estimation is strongly species-dependent (Fig. 2). The use of species-specific CHL_l-N_l ratios of leaves further complicates the remote sensing-based N_c estimation due to its dependence on local light climate. In this study, REGFLEC gave the best overall capabilities to predict N_c in all landscapes ($r^2 = 0.53$; rmse = 2.21 g m^{-2}). When applying

the simpler empirical-statistical SVI models jointly to all landscapes, N_c could be estimated with rmse in the range 2.4–2.8 g m^{-2}.

5.2 Remote sensing and carbon-nitrogen dynamics

The problem of scale is considered one of the largest challenges to provide robust global and European greenhouse gas budgets for croplands (Osborne et al., 2010). Current global estimates use plot scale determinations which may have only local or regional relevance or large-scale remote sensing techniques which do not resolve local or regional differences (Osborne et al., 2010). Even though remote sensing data are frequently used to assess chlorophyll and leaf nitrogen for crop precision management, methods are developed and tested using plot-scale data, and they are often considered to lack the required accuracy and precision to reflect temporal and/or spatial heterogenity for regional carbon budget modelling of croplands (e.g. Wattenback et al., 2010). The current study showed that high spatial resolution remote sensing of selected landscapes representing crop- and grasslands over a large gradient of environmental conditions in Europe can provide LAI predictions with a rmse of 0.73 (r^2 = 0.7), CHL_c predictions with rmse of 439 mg m^{-2} and N_c predictions with rmse of 2.2 g m^{-2} (r^2 = 0.53). Better results could be obtained when restricting regression model building to individual landscapes. These findings support the use of remote sensing data to characterize spatial variability in vegetation traits for regional carbon and nitrogen cycle modelling. Whereas well-instrumented experimental sites can deliver the data to parameterize plot- or field scale agro-ecosystem models, remote sensing-based estimates of LAI, CHL_c and N_c provide spatial information on ecophysiological conditions which can contribute to improve the realism and representation of site-specific effects of field management practice for regional modelling and upscaling of water, carbon and nitrogen cycling processes (e.g. Boegh et al., 2004, 2009; Houborg et al., 2007; Gitelson et al., 2009; Ciais et al., 2010). This paper demonstrated the capability of high

spatial resolution data to provide such input with statistical confidence for a subset of landscapes located over an extended region (Europe).

Leaf nitrogen is a key driver for biogeochemical cycling through its signficance for photosynthesis and respiration modelling (e.g. Boegh et al., 2002; Kattge et al., 2009), and it is also found to be important to assess the stomatal NH_3 compensation point, which determines whether vegetation canopies act as a source or a sink for NH_3 (Massad et al., 2008). In order to understand how nitrogen availability affects carbon and ammonia fluxes of ecosystems, N_l is clearly important. In a global study of leaf nitrogen variability (Freschet et al., 2011), it was found that as much as 50 % of the variability occurred *within* communities whereas 15 % occurred between communities and 35 % of global variance occurred between biomes. These results indicate that a significant part of global plant trait variation cannot be described using broad-scale influences (e.g. climate and topography) but that variations exist within plant communities at a fine spatial scale. High spatial resolution remote sensing data of LAI, CHL_c and N_c have potential to assess the spatial variability of plant functional traits, though methods still remain to be thoroughly verified for forest ecosystems, and to study the significance of such variability on the interacting carbon and nitrogen cycles.

While many natural ecosystems are nutrient-limited, the nitrogen balance of agricultural areas is generally positive in Europe. This means that there is a nitrogen surplus which contributes to nitrogen leaching, nitrous oxide emission (Schelde et al., 2012) and ammonia volatilization (Sutton et al., 2007). However, there are large variations within different European landscapes that are dependent on agricultural systems such as livestock production and the use of manure and inorganic fertilizers (e.g. Dalgaard et al., 2012). Since foliage N_l is closely related to nitrogen additions and soil mineral availability, as observed for forbs and grasses (Song et al., 2011), remote sensing-based N_c estimates may provide useful information to design field sampling strategies and adjust the simulations of agro-ecosystem models to partition deposited nitrogen between plants and soils. Vegetation (N_c or biomass) maps can also be used to assess spatial variation in nitrogen uptake of crop fields which is important for the soil

nitrogen balance. Together with measurements of nitrogen emissions and flows in landscapes, spatial information of biomass nitrogen pools are important to improve the understanding of nitrogen availability effects on the green house gas budget of terrestrial ecosystems (e.g. Schulze et al., 2010). In this study, biomass nitrogen pools varied widely within and between five European agricultural landscapes, with the lowest nitrogen pool found in the early-season DK09 landscape (64.72 t), and the largest pool found in PL (401.29 t) due to the larger proportion of agricultural area. Despite DK having the lowest proportional area of agricultural land, the second-highest nitrogen pool was found here (DK08, 31 May). The largest nitrogen concentrations within agricultural areas were found in DK08, IT and PL.

The hydrological cycle also has a critical impact on the greenhouse gas balance (e.g. Schulze et al., 2010). In this context, remote sensing can provide spatial information on vegetation development and ecophysiological condition to improve the regional simulation of evapotranspiration, photosynthesis and vegetation growth (e.g. Boegh et al., 2002b, 2004, 2009; Houborg et al., 2007, 2011; Peng and Gitelson, 2012). The current study indicates that high spatial resolution remote sensing-based estimates of LAI, CHL_c and N_c can be applied over extended regions with sufficient statistical confidence for such purposes. The sensitivity of model studies relative to the accuracy of remote sensing-based predictions should however be assessed.

With the launch of the upcoming European Sentinel-2 satellite mission (scheduled for 2013), 13 spectral bands should be available in the red-shortwave infrared at high spatial resolution (10–60 m) with three new bands located in the red-edge region. This would support the use of additional narrow bands with optimized sensitivity to changes in CHL_l and with reduced sensitivity to confounding factors. The availability of Sentinel-2 data would significantly advance the ability to monitor plant physiological condition both in terms of retrieval accuracy and spatio-temporal resolution (20 m every 2–5 days) using SVIs and a tool such as REGFLEC.

6 Conclusions

The capabilities of five SVIs (NDVI, SR, EVI2, GNDVI and CI) and the REGFLEC model were found to be statistically significant for LAI, CHL_c and N_c mapping when applied at high spatial resolution for five contrasting European crop- and grasslands. This strongly supports the applicability of such products to characterize spatial variability in vegetation traits for regional simulation and upscaling of water, carbon and nitrogen cycles.

The best results over the large range of environmental conditions represented by the five landscapes were achieved using an automatic spatial regularization technique (REGFLEC) to parameterize an image-based atmospheric-leaf optics-CRTM model (LAI rmse = 0.73; CHL_c rmse = 439 mg m^{-2}; N_c rmse = 2.2 g m^{-2}). The use of simpler SVI approaches also provided statistically significant results when calibrated against field data representing a variety of grasses and crop types, albeit with lower accuracies. Generally predictabilities improved when restricting the evaluation to separate land use categories, and they improved further when restricting the evaluation to local ($10 \times 10\,km^2$) landscapes, thereby reflecting sensitivity to canopy structures and local environmental conditions (i.e. soil background reflectance). At landscape scale, REGFLEC and the SVIs had different preditabilities. Combining the best methodologies for each landscape, improved predictabilities were achieved for LAI (rmse = 0.59), CHL_c (rmse = 346 mg m^{-2}) and N_c (rmse = 1.49 g m^{-2}) of the European agricultural landscapes which were comparable with or better than results reported in other studies using field spectrometric studies. One exception was for N_c for which much better predictabilities were found in field-spectrometric studies using narrow-band reflectance data. The N_c prediction is further complicted by a strong species-specific relationship between spectral leaf reflectance and N_l, as shown by the SPAD meter data in the current study.

Vertical CHL_l gradient profiles within canopies were found to reduce the predictability of remote sensing methods. The existence of vertical CHL_l gradient profiles violates the assumptions of CRTMs, including the ACRM used by REGFLEC, but also reduced

the predictability of SVIs. In order to establish an effective groundtruth reference data set for evaluating remote sensing-based predictions, canopies should be characterized by uniform CHL_l development. The current study used homogeneous canopies without positive or negative CHL_l vertical gradients as reference data to evaluate remote sensing predictions. In the future, field spectrometric studies should be designed to examine the effect of CHL_l vertical gradients on spectral canopy reflectance and remote sensing predictions of LAI, CHL_l and N_l.

Despite the demonstrated capability of REGFLEC to simulate CHL_l in previous studies, it was not possible to achieve statistically significant ($p < 0.05$) results for leaf scale predictions in this study. The ill-posed nature of the model inversion significantly complicates the process of extracting the CHL_l (and LAI) signal from remote sensing observations. The current study took place in the middle of the growing season, except for DK09 where REGFLEC results were best, and it is expected that the availability of an out-of-season satellite image with larger soil exposure would improve the results.

Results achieved in the current study for N_c prediction of European agricultural landscapes ($r^2 = 0.76$; rmse = 1.49) showed large spatial variations within and between landscapes which are attributed to seasonal variations, extent of agricultural area, different species, and spatial variation in nutrient availability. Such spatial information is important to improve understanding, modelling and upscaling of carbon and nitrogen budgets. With the launch of the European satellite mission Sentinel-2 in 2013, new narrow-band data opportunities are expected to improve the accuracies of LAI, CHL_l and N_l assessments. With these data, the mapping of seasonal variations in LAI, CHL_l and N_l with a high spatial resolution will be possible.

Acknowledgements. This study is a contribution to the EU Integrated Project NitroEurope (http://www.nitroeurope.eu), which was funded by the European Commision (project 17841-2), and to the project "Remote sensing of leaf nutrition and its incorporation for biochemical and environmental modelling of crop photosynthesis and evapotranspiration", funded by the Danish National Research Council (project 23-04-00156). The study is also affiliated to the project "Ecosystems Surface Exchange of Greenhouse Gases in an Environment of Changing Anthropogenic and Climatic Forcing" (ECOCLIM), financed by the Danish Strategic Research Council (project 10-093901). Financial support by Spot Image, now Astrium GeoInformation Services, to acquire SPOT satellite images is gratefully acknowledged. The authors would also like to acknowledge the European Commission for use of the ESDB soilmap, and we would like to acknowledge the use of free MODIS data downloaded from the NASA EOSDIS data center, ORNL-DAAC. Finally, but not least, we would like to thank the farmers and landowners within the NitroEurope landscapes for their kind collaboration and permissions to make measurements in their fields.

References

Astrium: The SPOT Satellites, available at: http://www.astrium-geo.com/en/192-the-spot-satellites (last access: 9 July 2012), 2012.

Atzberger, C. and Richter, K.: Spatially constrained inversion of radiative transfer models for improved lai mapping from future sentinel-2 imagery, Remote Sens. Environ., 120, 208–218, doi:10.1016/j.rse.2011.10.035, 2012.

Atzberger, C., Guerif, M., Baret, F., and Werner, W.: Comparative analysis of three chemometric techniques for the spectroradiometric assessment of canopy chlorophyll content in winter wheat, Comput. Electron. Agr., 73, 165–173, doi:10.1016/j.compag.2010.05.006, 2010.

Baret, F. and Fourty, T.: Radiometric estimates of nitrogen status in leaves and canopies, in: Diagnosis of the Nitrogen Status in Crops, edited by: Lemaire, G., Springer, Berlin, 201–227, 1997.

Blackburn, G. A.: Spectral indices for estimating photosynthetic pigment concentrations: a test using senescent tree leaves, Int. J. Remote Sens., 19, 657–675, doi:10.1080/014311698215919, 1998.

Boegh, E., Soegaard, H., Broge, N., Hasager, C. B., Jensen, N. O., Schelde, K., and Thomsen, A.: Airborne multispectral data for quantifying leaf area index, nitrogen concentration, and photosynthetic efficiency in agriculture, Remote Sens. Environ., 81, 179–193, doi:10.1016/s0034-4257(01)00342-x, 2002.

Boegh, E., Thorsen, M., Butts, M. B., Hansen, S., Christiansen, J. S., Abrahamsen, P., Hasager, C. B., Jensen, N. O., van der Keur, P., Refsgaard, J. C., Schelde, K., Soegaard, H., and Thomsen, A.: Incorporating remote sensing data in physically based distributed agro-hydrological modelling, J. Hydrol., 287, 279–299, doi:10.1016/j.jhydrol.2003.10.018, 2004.

Boegh, E., Poulsen, R. N., Butts, M., Abrahamsen, P., Dellwik, E., Hansen, S., Hasager, C. B., Ibrom, A., Loerup, J. K., Pilegaard, K., and Soegaard, H.: Remote sensing based evapotranspiration and runoff modeling of agricultural, forest and urban flux sites in Denmark: from field to macro-scale, J. Hydrol., 377, 300–316, doi:10.1016/j.jhydrol.2009.08.029, 2009.

Broge, N. H. and Leblanc, E.: Comparing prediction power and stability of broadband and hyperspectral vegetation indices for estimation of green leaf area index and canopy chlorophyll density, Remote Sens. Environ., 76, 156–172, doi:10.1016/s0034-4257(00)00197-8, 2001.

Carlson, T. N. and Ripley, D. A.: On the relation between ndvi, fractional vegetation cover, and leaf area index, Remote Sens. Environ., 62, 241–252, doi:10.1016/s0034-4257(97)00104-1, 1997.

Casa, R., Baret, F., Buis, S., Lopez-Lozano, R., Pascucci, S., Palombo, A., and Jones, H. G.: Estimation of maize canopy properties from remote sensing by inversion of 1-d and 4-d models, Precis. Agric., 11, 319–334, doi:10.1007/s11119-010-9162-9, 2010.

Cellier, P., Bleeker, A., Breuer, L., Dalgaard, T., Dragosits, U., Drouet, J. L., Durand, P., Duretz, S., Hutchings, N., Kros, J., Loubet, B., Oenema, O., Olesen, J. E., Mérot, P., Theobald, M. R., Viaud, V., de Vries, W., and Sutton, M. A.: Dispersion and fate of nitrogen in rural landscapes, Chapter 11, in: The European Nitrogen Assessment, edited by: Sutton, M. A., Howard, C. M., Erisman, J. W., Billen, G., Bleeker, A., Grennfelt, P., van Grinsven, H., and Grizzetti, B., Cambridge University Press, Cambridge, UK, 229–248, 2011.

Chen, T. X., van der Werf, G. R., Dolman, A. J., and Groenendijk, M.: Evaluation of cropland maximum light use efficiency using eddy flux measurements in North America and Europe, Geophys. Res. Lett., 38, L14707, doi:10.1029/2011gl047533, 2011.

Churkina, G., Zaehle, S., Hughes, J., Viovy, N., Chen, Y., Jung, M., Heumann, B. W., Ramankutty, N., Heimann, M., and Jones, C.: Interactions between nitrogen deposition, land cover conversion, and climate change determine the contemporary carbon balance of Europe, Biogeosciences, 7, 2749–2764, doi:10.5194/bg-7-2749-2010, 2010.

Ciais, P., Wattenbach, M., Vuichard, N., Smith, P., Piao, S. L., Don, A., Luyssaert, S., Janssens, I. A., Bondeau, A., Dechow, R., Leip, A., Smith, P. C., Beer, C., van der Werf, G. R., Gervois, S., Van Oost, K., Tomelleri, E., Freibauer, A., Schulze, E. D., and Team, C. S.: The European carbon balance. Part 2: Croplands, Global Change Biol., 16, 1409–1428, doi:10.1111/j.1365-2486.2009.02055.x, 2010.

Combal, B., Baret, F., Weiss, M., Trubuil, A., Mace, D., Pragnere, A., Myneni, R., Knyazikhin, Y., and Wang, L.: Retrieval of canopy biophysical variables from bidirectional reflectance – using prior information to solve the ill-posed inverse problem, Remote Sens. Environ., 84, 1–15, doi:10.1016/s0034-4257(02)00035-4, 2003.

Dalgaard, T., Bienkowski, J. F., Bleeker, A., Drouet, J. L., Durand, P., Dragosits, U., Frumau, A., Hutchings, N. J., Kedziora, A., Magliulo, V., Olesen, J. E., Theobald, M. R., Maury, O., Akkal, N., and Cellier, P.: Farm nitrogen balances in six European agricultural landscapes – a method for farming system assessment, emission hotspot identification, and mitigation measure evaluation, Biogeosciences Discuss., 9, 8859–8904, doi:10.5194/bgd-9-8859-2012, 2012.

Darvishzadeh, R., Skidmore, A., Schlerf, M., and Atzberger, C.: Inversion of a radiative transfer model for estimating vegetation lai and chlorophyll in a heterogeneous grassland, Remote Sens. Environ., 112, 2592–2604, doi:10.1016/j.rse.2007.12.003, 2008.

Dash, J., Curran, P. J., Tallis, M. J., Llewellyn, G. M., Taylor, G., and Snoeij, P.: Validating the meris terrestrial chlorophyll index (mtci) with ground chlorophyll content data at meris spatial resolution, Int. J. Remote Sens., 31, 5513–5532, doi:10.1080/01431160903376340, 2010.

de Pury, D. G. G. and Farquhar, G. D.: Simple scaling of photosynthesis from leaves to canopies without the errors of big-leaf models, Plant Cell Environ., 20, 537–557, doi:10.1111/j.1365-3040.1997.00094.x, 1997.

Duretz, S., Drouet, J. L., Durand, P., Hutchings, N. J., Theobald, M. R., Salmon-Monviola, J., Dragosits, U., Maury, O., Sutton, M. A., and Cellier, P.: Nitroscape: a model to integrate nitrogen transfers and transformations in rural landscapes, Environ. Pollut., 159, 3162–3170, doi:10.1016/j.envpol.2011.05.005, 2011.

EEA/ETC-LUS I: The European Environment – State and Outlook 2010, Land use, ISBN 978-92-9213-160-9, EEA, Copenhagen, 2010.

ESDB: Joint Research Centre, European Commission. European Soil Portal – Soil Data and Information Systems, available at: http://eusoils.jrc.ec.europa.eu/ESDB_Archive/ESDB/ (last access: 9 July 2012), 2010.

Eurostat: Nitrogen balance in agriculture, available at: http://www.ec.europa.eu/eurostat/ (last access: 9 July 2012), 2012.

Farquhar, G. D., Caemmerer, S. V., and Berry, J. A.: A biochemical-model of photosynthetic CO_2 assimilation in leaves of C-3 species, Planta, 149, 78–90, doi:10.1007/bf00386231, 1980.

Field, C. B., Randerson, J. T., and Malmstrom, C. M.: Global net primary production – combining ecology and remote-sensing, Remote Sens. Environ., 51, 74–88, doi:10.1016/0034-4257(94)00066-v, 1995.
Filella, I., Serrano, L., Serra, J., and Penuelas, J.: Evaluating wheat nitrogen status with canopy reflectance indexes and discriminant-analysis, Crop Sci., 35, 1400–1405, 1995.
Fitzgerald, G., Rodriguez, D., and O'Leary, G.: Measuring and predicting canopy nitrogen nutrition in wheat using a spectral index-the canopy chlorophyll content index (ccci), Field Crop. Res., 116, 318–324, doi:10.1016/j.fcr.2010.01.010, 2010.
Freschet, G. T., Dias, A. T. C., Ackerly, D. D., Aerts, R., van Bodegom, P. M., Cornwell, W. K., Dong, M., Kurokawa, H., Liu, G. F., Onipchenko, V. G., Ordonez, J. C., Peltzer, D. A., Richardson, S. J., Shidakov, II, Soudzilovskaia, N. A., Tao, J. P., and Cornelissen, J. H. C.: Global to community scale differences in the prevalence of convergent over divergent leaf trait distributions in plant assemblages, Global Ecol. Biogeogr., 20, 755–765, doi:10.1111/j.1466-8238.2011.00651.x, 2011.
Garrigues, S., Lacaze, R., Baret, F., Morisette, J. T., Weiss, M., Nickeson, J. E., Fernandes, R., Plummer, S., Shabanov, N. V., Myneni, R. B., Knyazikhin, Y., and Yang, W.: Validation and intercomparison of global leaf area index products derived from remote sensing data, J. Geophys. Res.-Biogeo., 113, G02028, doi:10.1029/2007jg000635, 2008.
Gitelson, A. A., Kaufman, Y. J., and Merzlyak, M. N.: Use of a green channel in remote sensing of global vegetation from eos-modis, Remote Sens. Environ., 58, 289–298, doi:10.1016/s0034-4257(96)00072-7, 1996.
Gitelson, A. A., Vina, A., Ciganda, V., Rundquist, D. C., and Arkebauer, T. J.: Remote estimation of canopy chlorophyll content in crops, Geophys. Res. Lett., 32, L08403, doi:10.1029/2005gl022688, 2005.
Godin, C. and Sinoquet, H.: Functional-structural plant modelling, New Phytol., 166, 705–708, doi:10.1111/j.1469-8137.2005.01445.x, 2005.
Haboudane, D., Miller, J. R., Pattey, E., Zarco-Tejada, P. J., and Strachan, I. B.: Hyperspectral vegetation indices and novel algorithms for predicting green lai of crop canopies: modeling and validation in the context of precision agriculture, Remote Sens. Environ., 90, 337–352, doi:10.1016/j.rse.2003.12.013, 2004.
Hallik, L., Niinemets, U., and Kull, O.: Photosynthetic acclimation to light in woody and herbaceous species: a comparison of leaf structure, pigment content and chlorophyll fluorescence characteristics measured in the field, Plant Biol., 14, 88–99, doi:10.1111/j.1438-8677.2011.00472.x, 2012.
Hansen, P. M. and Schjoerring, J. K.: Reflectance measurement of canopy biomass and nitrogen status in wheat crops using normalized difference vegetation indices and partial least squares regression, Remote Sens. Environ., 86, 542–553, doi:10.1016/s0034-4257(03)00131-7, 2003.
Houborg, R. and Anderson, M. C.: Utility of an image-based canopy reflectance modeling tool for remote estimation of lai and leaf chlorophyll content at regional scales, J. Appl. Remote Sens., 3, 033529, doi:10.1117/1.3141522, 2009.
Houborg, R., Anderson, M. C., Daughtry, C. S. T., Kustas, W. P., and Rodell, M.: Using leaf chlorophyll to parameterize light-use-efficiency within a thermal-based carbon, water and energy exchange model, Remote Sens. Environ., 115, 1694–1705, doi:10.1016/j.rse.2011.02.027, 2011.
Huete, A., Didan, K., Miura, T., Rodriguez, E. P., Gao, X., and Ferreira, L. G.: Overview of the radiometric and biophysical performance of the modis vegetation indices, Remote Sens. Environ., 83, 195–213, doi:10.1016/s0034-4257(02)00096-2, 2002.
Huete, A. R.: A soil-adjusted vegetation index (SAVI), Remote Sens. Environ., 25, 295–309, doi:10.1016/0034-4257(88)90106-x, 1988.
Huete, A. R., Didan, K., Shimabukuro, Y. E., Ratana, P., Saleska, S. R., Hutyra, L. R., Yang, W. Z., Nemani, R. R., and Myneni, R.: Amazon rainforests green-up with sunlight in dry season, Geophys. Res. Lett., 33, L06405, doi:10.1029/2005gl025583, 2006.
Jacquemoud, S. and Baret, F.: Prospect – a model of leaf optical-properties spectra, Remote Sens. Environ., 34, 75–91, doi:10.1016/0034-4257(90)90100-z, 1990.
Jacquemoud, S., Bacour, C., Poilve, H., and Frangi, J. P.: Comparison of four radiative transfer models to simulate plant canopies reflectance: direct and inverse mode, Remote Sens. Environ., 74, 471–481, doi:10.1016/s0034-4257(00)00139-5, 2000.
Jiang, Z. Y., Huete, A. R., Didan, K., and Miura, T.: Development of a two-band enhanced vegetation index without a blue band, Remote Sens. Environ., 112, 3833–3845, doi:10.1016/j.rse.2008.06.006, 2008.
Jung, M., Vetter, M., Herold, M., Churkina, G., Reichstein, M., Zaehle, S., Ciais, P., Viovy, N., Bondeau, A., Chen, Y., Trusilova, K., Feser, F., and Heimann, M.: Uncertainties of modeling gross primary productivity over europe: a systematic study on the effects of using

different drivers and terrestrial biosphere models, Global Biogeochem. Cy., 21, Gb4021, doi:10.1029/2006gb002915, 2007.
Kattge, J., Knorr, W., Raddatz, T., and Wirth, C.: Quantifying photosynthetic capacity and its relationship to leaf nitrogen content for global-scale terrestrial biosphere models, Global Change Biol., 15, 976–991, doi:10.1111/j.1365-2486.2008.01744.x, 2009.
Knyazikhin, Y., Martonchik, J. V., Myneni, R. B., Diner, D. J., and Running, S. W.: Synergistic algorithm for estimating vegetation canopy leaf area index and fraction of absorbed photosynthetically active radiation from modis and misr data, J. Geophys. Res.-Atmos., 103, 32257–32275, doi:10.1029/98jd02462, 1998.
Kotchenova, S. Y., Vermote, E. F., Matarrese, R., and Klemm, F. J.: Validation of a vector version of the 6s radiative transfer code for atmospheric correction of satellite data. Part I: Path radiance, Appl. Optics, 45, 6762–6774, doi:10.1364/ao.45.006762, 2006.
Kuusk, A.: A two-layer canopy reflectance model, J. Quant. Spectrosc. Ra., 71, 1–9, doi:10.1016/s0022-4073(01)00007-3, 2001.
Main, R., Cho, M. A., Mathieu, R., O'Kennedy, M. M., Ramoelo, A., and Koch, S.: An investigation into robust spectral indices for leaf chlorophyll estimation, ISPRS J. Photogramm., 66, 751–761, doi:10.1016/j.isprsjprs.2011.08.001, 2011.
Massad, R. S., Tuzet, A., Loubet, B., Perrier, A., and Cellier, P.: Model of stomatal ammonia compensation point (stamp) in relation to the plant nitrogen and carbon metabolisms and environmental conditions, Ecol. Model., 221, 479–494, doi:10.1016/j.ecolmodel.2009.10.029, 2010.
Mattsson, M., Herrmann, B., David, M., Loubet, B., Riedo, M., Theobald, M. R., Sutton, M. A., Bruhn, D., Neftel, A., and Schjoerring, J. K.: Temporal variability in bioassays of the stomatal ammonia compensation point in relation to plant and soil nitrogen parameters in intensively managed grassland, Biogeosciences, 6, 171–179, doi:10.5194/bg-6-171-2009, 2009.
Moors, E. J., Jacobs, C., Jans, W., Supit, I., Kutsch, W. L., Bernhofer, C., Beziat, P., Buchmann, N., Carrara, A., Ceschia, E., Elbers, J., Eugster, W., Kruijt, B., Loubet, B., Magliulo, E., Moureaux, C., Olioso, A., Saunders, M., and Soegaard, H.: Variability in carbon exchange of european croplands, Agr. Ecosyst. Environ., 139, 325–335, doi:10.1016/j.agee.2010.04.013, 2010.
Osborne, B., Saunders, M., Walmsley, D., Jones, M., and Smith, P.: Key questions and uncertainties associated with the assessment of the cropland greenhouse gas balance, Agr. Ecosyst. Environ., 139, 293–301, doi:10.1016/j.agee.2010.05.009, 2010.

Peel, M. C., Finlayson, B. L., and McMahon, T. A.: Updated world map of the Köppen-Geiger climate classification, Hydrol. Earth Syst. Sci., 11, 1633–1644, doi:10.5194/hess-11-1633-2007, 2007.
Peng, Y. and Gitelson, A. A.: Remote estimation of gross primary productivity in soybean and maize based on total crop chlorophyll content, Remote Sens. Environ., 117, 440–448, doi:10.1016/j.rse.2011.10.021, 2012.
Porra, R. J., Thompson, W. A., and Kriedemann, P. E.: Determination of accurate extinction coefficients and simultaneous-equations for assaying chlorophyll *a* and chlorophyll *b* extracted with 4 different solvents – verification of the concentration of chlorophyll standards by atomic-absorption spectroscopy, Biochim. Biophys. Acta, 975, 384–394, doi:10.1016/s0005-2728(89)80347-0, 1989.
Schelde, K., Cellier, P., Bertolini, T., Dalgaard, T., Weidinger, T., Theobald, M. R., and Olesen, J. E.: Nitrous oxide emissions at the landscape scale: spatial and temporal variability, Biogeosciences Discuss., 8, 11941–11978, doi:10.5194/bgd-8-11941-2011, 2011.
Schulze, E. D., Ciais, P., Luyssaert, S., Schrumpf, M., Janssens, I. A., Thiruchittampalam, B., Theloke, J., Saurat, M., Bringezu, S., Lelieveld, J., Lohila, A., Rebmann, C., Jung, M., Bastviken, D., Abril, G., Grassi, G., Leip, A., Freibauer, A., Kutsch, W., Don, A., Nieschulze, J., Borner, A., Gash, J. H., and Dolman, A. J.: The european carbon balance. Part 4: Integration of carbon and other trace-gas fluxes, Global Change Biol., 16, 1451–1469, doi:10.1111/j.1365-2486.2010.02215.x, 2010.
Sims, D. A. and Gamon, J. A.: Relationships between leaf pigment content and spectral reflectance across a wide range of species, leaf structures and developmental stages, Remote Sens. Environ., 81, 337–354, doi:10.1016/s0034-4257(02)00010-x, 2002.
Song, L., Bao, X., Liu, X., Zhang, Y., Christie, P., Fangmeier, A., and Zhang, F.: Nitrogen enrichment enhances the dominance of grasses over forbs in a temperate steppe ecosystem, Biogeosciences, 8, 2341–2350, doi:10.5194/bg-8-2341-2011, 2011.
Sutton, M. A., Nemitz, E., Erisman, J. W., Beier, C., Bahl, K. B., Cellier, P., de Vries, W., Cotrufo, F., Skiba, U., Di Marco, C., Jones, S., Laville, P., Soussana, J. F., Loubet, B., Twigg, M., Famulari, D., Whitehead, J., Gallagher, M. W., Neftel, A., Flechard, C. R., Herrmann, B., Calanca, P. L., Schjoerring, J. K., Daemmgen, U., Horvath, L., Tang, Y. S., Emmett, B. A., Tietema, A., Penuelas, J., Kesik, M., Brueggemann, N., Pilegaard, K., Vesala, T., Campbell, C. L., Olesen, J. E., Dragosits, U., Theobald, M. R., Levy, P., Mobbs, D. C., Milne, R., Viovy, N., Vuichard, N., Smith, J. U., Smith, P., Bergamaschi, P., Fowler, D., and

Reis, S.: Challenges in quantifying biosphere-atmosphere exchange of nitrogen species, Environ. Pollut., 150, 125–139, doi:10.1016/j.envpol.2007.04.014, 2007.
Verhoef, W. and Bach, H.: Simulation of sentinel-3 images by four-stream surface-atmosphere radiative transfer modeling in the optical and thermal domains, Remote Sens. Environ., 120, 197–207, doi:10.1016/j.rse.2011.10.034, 2012.
Vermote, E. F., ElSaleous, N., Justice, C. O., Kaufman, Y. J., Privette, J. L., Remer, L., Roger, J. C., and Tanre, D.: Atmospheric correction of visible to middle-infrared eos-modis data over land surfaces: background, operational algorithm and validation, J. Geophys. Res.-Atmos., 102, 17131–17141, doi:10.1029/97jd00201, 1997.
Vina, A., Gitelson, A. A., Nguy-Robertson, A. L., and Peng, Y.: Comparison of different vegetation indices for the remote assessment of green leaf area index of crops, Remote Sens. Environ., 115, 3468–3478, doi:10.1016/j.rse.2011.08.010, 2011.
Wattenbach, M., Sus, O., Vuichard, N., Lehuger, S., Gottschalk, P., Li, L. H., Leip, A., Williams, M., Tomelleri, E., Kutsch, W. L., Buchmann, N., Eugster, W., Dietiker, D., Aubinet, M., Ceschia, E., Beziat, P., Grunwald, T., Hastings, A., Osborne, B., Ciais, P., Cellier, P., and Smith, P.: The carbon balance of european croplands: a cross-site comparison of simulation models, Agr. Ecosyst. Environ., 139, 419–453, doi:10.1016/j.agee.2010.08.004, 2010.
Winterhalter, L., Mistele, B., and Schmidhalter, U.: Assessing the vertical footprint of reflectance measurements to characterize nitrogen uptake and biomass distribution in maize canopies, Field Crop. Res., 129, 14–20, doi:10.1016/j.fcr.2012.01.007, 2012.
Yoder, B. J. and Pettigrewcrosby, R. E.: Predicting nitrogen and chlorophyll content and concentrations from reflectance spectra (400–2500 nm) at leaf and canopy scales, Remote Sens. Environ., 53, 199–211, doi:10.1016/0034-4257(95)00135-n, 1995.
Yoder, B. J. and Waring, R. H.: The normalized difference vegetation index of small douglas-fir canopies with varying chlorophyll concentrations, Remote Sens. Environ., 49, 81–91, doi:10.1016/0034-4257(94)90061-2, 1994.
Zhao, D. L., Reddy, K. R., Kakani, V. G., and Reddy, V. R.: Nitrogen deficiency effects on plant growth, leaf photosynthesis, and hyperspectral reflectance properties of sorghum, Eur. J. Agron., 22, 391–403, doi:10.1016/j.eja.2004.06.005, 2005.
Zhao, M. S., Heinsch, F. A., Nemani, R. R., and Running, S. W.: Improvements of the modis terrestrial gross and net primary production global data set, Remote Sens. Environ., 95, 164–176, doi:10.1016/j.rse.2004.12.011, 2005.

Table 1. Overview of SPOT satellite data including geographical, sensor and atmospheric data estimated from MODIS and AIRS satellite data. Atmospheric data include aerosol optical depth (τ), ozone content (O_3) and total precipitable water content (TPW). Spatial resolutions (Δx) of the SPOT images are also shown.

Country	Site acronym	Latitude (° N)	Longitude (° E)	Elevation (m.a.s.)	SPOT Date	SPOT Time (h)	SPOT Satellite	SPOT Sensor	SPOT Δx (m)	MODIS Time (h)	MODIS τ (–)	AIRS Time (h)	AIRS O_3 (Dobson)	AIRS TPW (kg m^{-2})
Denmark	DK08	56.34	9.66	60	31 May 2008	10.50	SPOT-4	HRVIR1	20	11.10	0.234	11.25	322.8	18.82
Poland	PL	52.04	16.78	80	1 Jun 2008	10.20	SPOT-4	HRG1	10	10.20	0.177	12.06	353.4	15.43
Netherlands	NL	53.14	6.13	2	9 Jun 2008	10.46	SPOT-5	HRG2	10	11.05	0.091	11.19	327.9	22.95
Italy	IT	40.51	14.94	15	27 Jun 2008	10.03	SPOT-5	HRG1	10	9.20	0.459	11.30	340.6	27.20
Scotland	UK	55.78	−3.24	280	21 Jul 2008	11.09	SPOT-4	HRVIR1	20	11.55	0.021	11.55	330.0	15.00
Denmark	DK09	56.35	9.66	60	17 Apr 2009	10.45	SPOT-5	HRG1	10	11.55	0.053	12.11	385.5	10.36

Table 2. Number of field plots and vegetation types represented by field measurements in the landscape sites.

Site	*n*	Vegetation types
DK08	20	winter wheat, barley, maize
DK09	22	winter wheat, winter oilseed rape
NL	22	grass, maize
PL	13	maize, barley, alfalfa, potatoes, rye, oilseed rape
IT	9	maize, tomato, arthichoke, alfalfa
UK	7	grass, wheat
all	93	

Table 3. Means and standard deviations (sd) of SPOT NDVI for the crop- and grasslands, measured leaf area index (LAI), leaf chlorophyll density (CHL_l), leaf nitrogen density (N_l), canopy chlorophyll density (CHL_c) and canopy nitrogen density (N_c) within the European landscape sites. Standard deviations of leaf scale measurements are shown to represent between-field variability (sd1) which is the "standard deviation of the mean CHL_l or N_l of different fields" and within-field variability (sd2) which is the averaged "CHL_l or N_l standard deviation of data measured in individual fields".

	NDVI mean (–)	NDVI sd (–)	LAI mean (–)	LAI sd (–)	CHL_l mean ($mg\,m^{-2}$)	CHL_l sd1 ($mg\,m^{-2}$)	CHL_l sd2 ($mg\,m^{-2}$)	N_l mean ($g\,m^{-2}$)	N_l sd1 ($g\,m^{-2}$)	N_l sd2 ($g\,m^{-2}$)	CHL_c mean ($mg\,m^{-2}$)	CHL_c sd1 ($mg\,m^{-2}$)	N_c mean ($g\,m^{-2}$)	N_c sd1 ($g\,m^{-2}$)
DK08	0.73	0.34	2.9	1.4	391	78	105	2.13	0.33	0.47	1095	588	6.10	3.24
DK09	0.72	0.39	2.2	1.1	434	96	164	2.27	0.19	0.24	1041	733	4.97	2.37
NL	0.73	0.34	3.0	1.5	350	121	121	1.71	0.23	0.22	1037	698	5.12	3.15
PL	0.67	0.42	2.1	1.1	402	102	67	2.27	0.97	0.35	832	633	5.10	5.36
IT	0.49	0.42	2.0*	0.7*	647	151	131	4.20	2.87	0.45	1370*	498*	5.51*	2.92*
UK	0.74	0.3	1.8	1.9	–	–	–	1.11	0.44	–	–	–	2.52	3.38

* Tomato fields not included.

Table 4. Determination coefficients (r^2) and root mean square errors (rmse) quantifying the capability of REGFLEC and SVIs (NDVI, SR, EVI2, GNDVI, CI) to estimate LAI, total canopy chlorophyll content (CHL_c) and total canopy nitrogen content (N_c) of distinct vegetation classes across the European landscape sites. The evaluations are using data from homogeneous canopies without strong CHL_l profile development. Number of observations (n), and the mean and standard deviation (sd) of these field data are also shown. Bold numbers indicate statistically significant ($p < 0.05$) results, and the superscripts symbolize the type of regression equation (l = linear; e = exponential). Italic numbers highlight the best predictabilities for each vegetation class and objective.

	n	data mean	data sd	NDVI r^2	NDVI rmse	SR r^2	SR rmse	EVI2 r^2	EVI2 rmse	GNDVI r^2	GNDVI rmse	CI r^2	CI rmse	REGFLEC r^2	REGFLEC rmse
LAI (–)															
All	72	2.38	1.35	**0.39**^{l}	1.04	**0.56**^{l}	0.89	**0.50**^{l}	0.95	**0.43**^{e}	0.99	**0.52**^{l}	0.93	***0.70***^{l}	0.73
Wheat	27	2.69	1.8	**0.43**^{e}	1.00	**0.39**^{e}	1.03	**0.47**^{l}	0.92	**0.41**^{e}	1.02	**0.40**^{e}	1.03	***0.75***^{l}	0.63
Grass	20	2.53	1.71	**0.63**^{l}	1.01	**0.75**^{l}	0.83	**0.61**^{l}	1.05	***0.83***^{e}	0.74	**0.79**^{l}	0.76	**0.78**^{l}	0.78
Maize	10	1.34	0.79	**0.57**^{l}	0.49	**0.63**^{l}	0.46	***0.80***^{l}	0.33	0.54^{l}	0.51	**0.62**^{l}	0.46	**0.78**^{l}	0.35
Barley	7	2.53	0.87	**0.68**^{e}	0.52	0.63^{l}	0.49	0.61^{e}	0.57	0.63^{l}	0.49	***0.70***^{l}	0.44	0.52^{l}	0.56
CHL_c (mg m^{-2})															
All	61	1021	631	**0.28**^{e}	552	**0.40**^{l}	487	**0.35**^{e}	497	**0.29**^{e}	548	**0.38**^{l}	494	***0.51***^{l}	439
Wheat	24	993	507	0.27^{l}	423	**0.28**^{l}	422	0.32^{l}	408	**0.36**^{l}	398	**0.40**^{l}	385	***0.66***^{l}	290
Grass	15	1126	696	**0.67**^{e}	415	**0.73**^{e}	369	**0.68**^{e}	400	**0.69**^{e}	393	**0.73**^{e}	370	***0.91***^{l}	201
Maize	9	687	487	0.34^{l}	372	0.29^{l}	386	0.40^{e}	481	0.37^{l}	365	0.35^{l}	369	*0.41*^{l}	353
Barley	6	925	349	**0.79**^{e}	176	**0.86**^{e}	136	**0.70**^{e}	204	**0.85**^{e}	151	***0.90***^{e}	117	**0.83**^{l}	130
N_c (g m^{-2})															
All	68	5.03	3.13	**0.23**^{e}	2.79	**0.40**^{l}	2.41	**0.30**^{l}	2.6	**0.30**^{e}	2.63	**0.42**^{l}	2.37	***0.53***^{l}	2.21
Wheat	26	5.79	2.65	**0.36**^{e}	2.14	**0.34**^{l}	2.1	**0.36**^{e}	2.28	**0.39**^{e}	2.02	**0.42**^{l}	1.98	***0.67***^{l}	2.38
Grass	20	4.37	3.41	**0.59**^{l}	2.12	**0.75**^{l}	1.68	**0.52**^{l}	2.29	**0.76**^{e}	1.45	**0.78**^{l}	1.56	***0.81***^{l}	1.68
Maize	9	2.03	1.16	**0.54**^{l}	0.74	**0.53**^{l}	0.75	***0.66***^{l}	0.63	**0.55**^{l}	0.73	**0.58**^{l}	0.71	**0.62**^{l}	1.03
Barley	6	5.42	1.97	**0.78**^{e}	0.96	**0.85**^{e}	0.77	**0.69**^{e}	1.15	**0.85**^{e}	0.78	***0.91***^{e}	0.59	**0.85**^{l}	1.82

Table 5. Determination coefficients (r^2) and root mean square errors (rmse) quantifying the capability of REGFLEC and SVIs (NDVI, SR, EVI2, GNDVI, CI) to estimate LAI, total canopy chlorophyll content (CHL_c) and total canopy nitrogen content (N_c) of different European landscapes. The evaluations are using data from homogeneous canopies without strong CHL_l profile development. Number of observations (n), and the mean and standard deviation (sd) of these field data are also shown. Bold numbers indicate statistically significant ($p < 0.05$) results, and the superscripts symbolize the type of regression equation (l = linear; e = exponential). Italic numbers highlight the best predictabilities for each landscape and objective.

	n	data mean	data sd	NDVI r^2	NDVI rmse	SR r^2	SR rmse	EVI2 r^2	EVI2 rmse	GNDVI r^2	GNDVI rmse	CI r^2	CI rmse	REGFLEC r^2	REGFLEC rmse
LAI (–)															
DK08	14	2.85	1.38	**0.93**^{e}	0.56	**0.85**^{l}	0.52	***0.94***^{e}	0.64	**0.93**^{e}	0.56	**0.83**^{l}	0.55	**0.79**^{l}	0.60
DK09	21	2.24	1.06	**0.59**^{e}	0.78	**0.58**^{e}	0.73	**0.69**^{e}	0.68	**0.62**^{e}	0.74	**0.63**^{e}	0.70	***0.74***^{l}	0.53
UK	7	1.78	1.89	**0.86**^{e}	0.60	**0.88**^{l}	0.62	***0.95***^{e}	0.31	**0.93**^{e}	0.76	**0.88**^{e}	1.20	**0.88**^{l}	0.61
PL	10	1.91	0.86	**0.79**^{e}	0.39	**0.77**^{l}	0.39	**0.77**^{e}	0.45	***0.82***^{e}	0.38	**0.76**^{l}	0.40	**0.70**^{l}	0.45
NL	16	2.99	1.58	**0.78**^{e}	0.83	**0.81**^{e}	0.74	***0.86***^{e}	0.67	**0.80**^{e}	0.80	**0.82**^{e}	0.73	**0.82**^{l}	0.65
IT	6	1.89	0.63	**0.82**^{l}	0.24	***0.85***^{l}	0.22	**0.73**^{e}	0.30	**0.79**^{e}	0.26	**0.79**^{e}	0.29	0.29^{l}	0.48
CHL_c (mg m^{-2})															
DK08	12	1087	590	***0.94***^{l}	247	**0.84**^{l}	223	***0.94***^{e}	273	***0.94***^{e}	247	**0.81**^{l}	246	**0.87**^{l}	207
DK09	20	1070	739	**0.39**^{e}	588	**0.41**^{e}	573	***0.70***^{l}	397	**0.48**^{e}	550	**0.50**^{l}	527	**0.66**^{l}	418
UK	0	–	–	–	–	–	–	–	–	–	–	–	–	–	–
PL	9	696	332	0.57^{e}	216	0.55^{l}	211	0.57^{e}	225	***0.61***^{e}	216	0.55^{e}	225	0.48^{l}	226
NL	16	1080	697	**0.67**^{e}	419	***0.75***^{e}	358	**0.67**^{e}	405	**0.65**^{e}	416	**0.73**^{e}	364	**0.71**^{l}	366
IT	6	1280	739	0.50^{l}	298	*0.55*^{l}	282	0.29^{l}	355	0.40^{l}	338	0.43^{l}	320	0.18^{l}	383
N_c (g m^{-2})															
DK08	12	6.05	3.20	***0.95***^{e}	1.12	**0.88**^{l}	1.07	***0.95***^{l}	1.33	**0.94**^{e}	1.21	**0.85**^{l}	1.20	**0.87**^{l}	2.49
DK09	20	5.68	2.88	**0.41**^{l}	2.16	**0.46**^{l}	2.07	**0.70**^{l}	1.55	**0.46**^{e}	2.02	**0.50**^{l}	1.90	***0.77***^{l}	1.93
UK	7	2.52	3.38	**0.83**^{e}	1.61	**0.90**^{e}	1.30	***0.91***^{e}	1.32	**0.86**^{e}	1.74	**0.90**^{e}	1.58	***0.91***^{l}	4.37
PL	9	3.72	2.44	0.40^{e}	1.97	0.36^{e}	1.95	0.42^{e}	1.99	*0.47*^{e}	1.93	0.39^{e}	1.99	0.21^{l}	1.98
NL	16	5.36	3.07	**0.79**^{e}	1.52	**0.82**^{e}	1.26	***0.85***^{e}	1.25	**0.82**^{e}	1.45	**0.84**^{e}	1.26	**0.83**^{l}	1.63
IT	6	5.30	3.32	0.14^{l}	2.82	0.12^{l}	2.85	*0.40*^{e}	2.35	0.21^{e}	3.01	0.17^{l}	2.77	0.00^{l}	5.28

Table 6. Percentage agricultural area (*A*), remote sensing based estimates of the average canopy nitrogen content (N_c) of agricultural regions, and the total N_c of the agricultural region within each of the 10 × 10 km^2 landscape sites.

	A (%)	N_c (g m^{-2})	N_c (t)
DK08	48	5.93	307.33
DK09	48	1.40	64.72
UK	77	1.43	110.56
PL	78	5.14	401.29
NL	69	4.04	277.97
IT	49	5.91	198.34

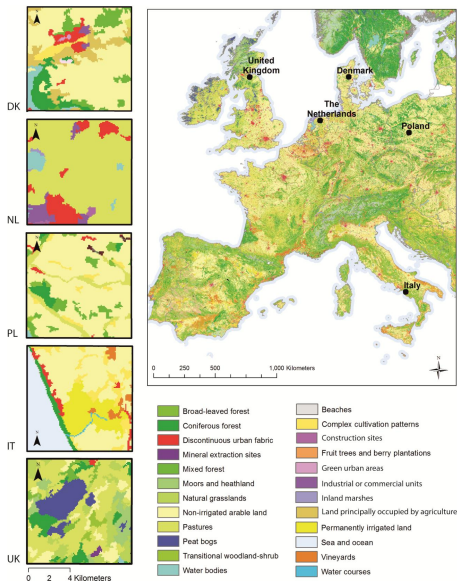

Fig. 1. Land cover and locations of 5 European landscape sites. Courtesy: CORINE land cover (CLC2000), European Environment Agency. (http://www.eea.europa.eu/legal/copyright).

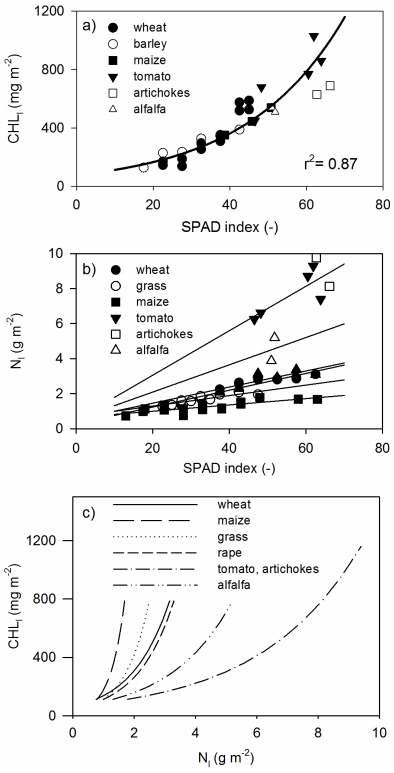

Fig. 2. SPAD meter calibration curves for **(a)** leaf chlorophyll (CHL_l) and **(b)** leaf nitrogen density (N_l), and **(c)** empirical relationships between N_l and CHL_l derived by combining SPAD calibration equations for CHL_l and N_l.

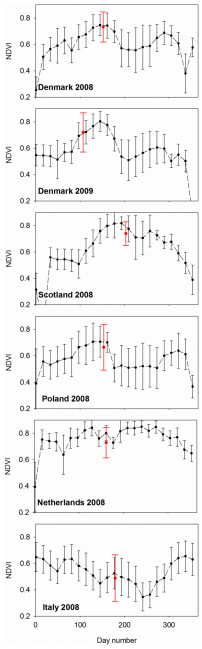

Fig. 3. Time series of average and standard deviation of NDVI for the agricultural area of each landscape extracted from MODIS data. The average and standard deviation NDVI calculated from each SPOT image of the agricultural region of NitroEurope landscapes is also shown. Due to different spatial resolutions of land use maps used for masking non-agricultural areas (1 km for MODIS), SPOT NDVI and MODIS NDVI are not representing exactly same areas.

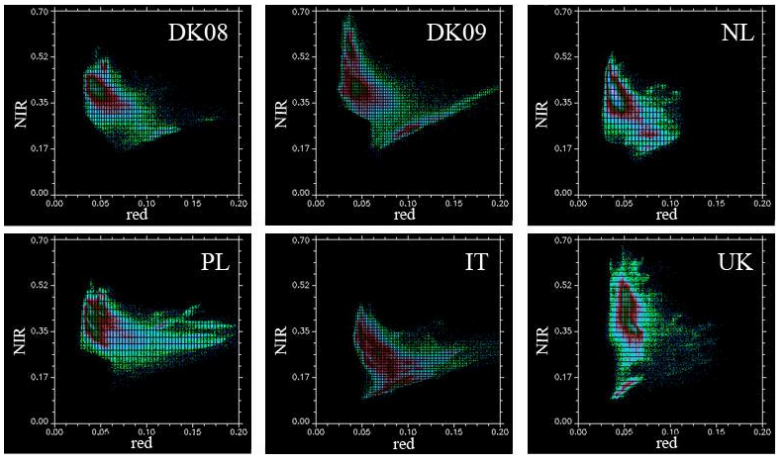

Fig. 4. Density scatterplots of nearinfrared (NIR) versus red surface reflectance of crop and grassland areas within each of the landscape sites calculated from SPOT satellite data.

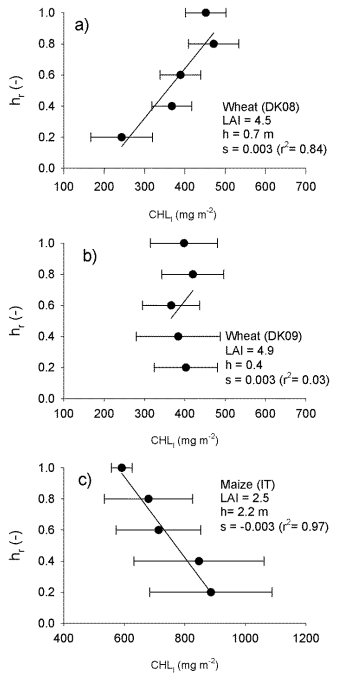

Fig. 5. Examples of three different characteristic vertical leaf chlorophyll (CHL_l) profiles based on field measurements within the studied landscape sites. The plots show mean and standard deviation CHL_l at relative measurement heights (h_r = measurement height divided by canopy height) and linear regression lines. Leaf area index (LAI), canopy height (h), and the slope (s) and determination coefficient (r^2) of linear regression slopes are indicated in each graph. Note that the slope in **(b)** is not statistically significant.

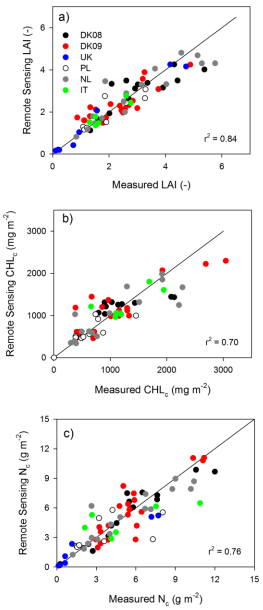

Fig. 6. Comparison of field measurements and remote sensing-based estimates of **(a)** leaf area index (LAI), **(b)** canopy chlorophyll content (CHL_c) and **(c)** canopy nitrogen content (N_c) of homogeneous canopies without strong chlorophyll vertical profile development. The remote sensing-based estimates for each landscape are based on the methods that were best correlated with the field measurements. Correlation coefficients representing predictability for individual countries are shown in Table 5.

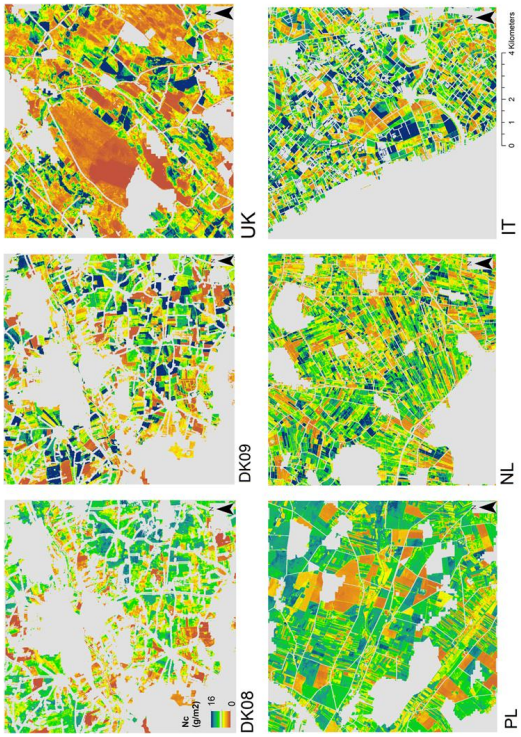

Fig. 7. Remote sensing-based maps of canopy nitrogen contents (N_c) of NitroEurope agricultural landscape sites located in Denmark (DK08, DK09), Scotland (UK), Poland (PL), the Netherlands (NL) and Italy (IT). Colour legend is shown in the DK08 image. Water, urban/suburban (incl streets) and forest areas are shown in grey. Frequency distributions of N_c are shown in Fig. 8.

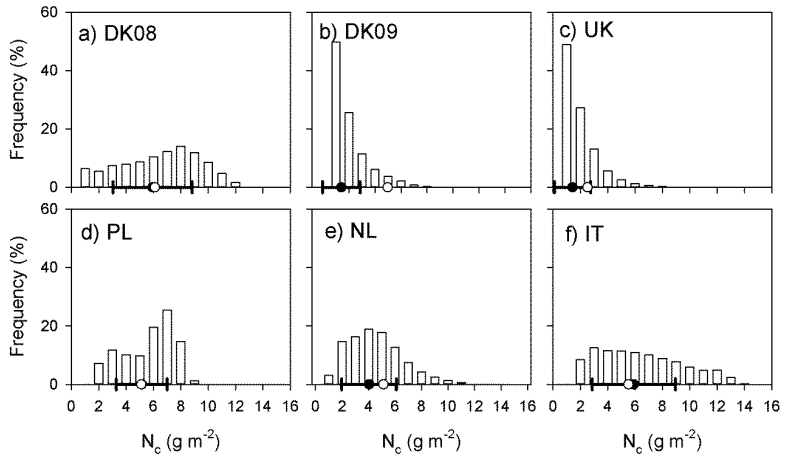

Fig. 8. Frequency distributions of canopy nitrogen (N_c) contents of crop- and grasslands in NitroEurope landscapes (mapped in Fig. 7) estimated using remote sensing for the **(a)** Danish site, 31 May 2008, **(b)** Danish site, 19 April 2009, **(c)** Scottish site, 21 July 2008, **(d)** Polish site, 1 June 2008, **(e)** Dutch site, 9 June 2008 and **(f)** Italian site, 27 June 2008. The means of field measurements are also indicated (white dot), and the mean and standard deviation of the remote sensing based estimations are shown (black dot).